Editors' Suggestion

Polarons free from many-body self-interaction in density functional theory

Stefano Falletta* and Alfredo Pasquarello

Chaire de Simulation à l'Echelle Atomique (CSEA), Ecole Polytechnique Fédérale de Lausanne (EPFL), CH-1015 Lausanne, Switzerland

(Received 10 May 2022; accepted 22 August 2022; published 14 September 2022)

We develop a unified theoretical framework encompassing one-body and many-body forms of self-interaction. We find an analytic expression for both the one-body and the many-body self-interaction energies, and quantitatively connect the two expressions through the dielectric constant. The two forms of self-interaction are found to coincide in the absence of electron screening. This analysis confers superiority to the notion of many-body self-interaction over the notion of one-body self-interaction. Next, we develop a semilocal density functional scheme that addresses the many-body self-interaction of polarons, thereby overcoming the limitations of standard density functional theory. Polaron localization is achieved through the addition of a weak local potential in the Kohn-Sham Hamiltonian that enforces the piece-wise linearity of the total energy upon partial electron occupation. Our method equivalently applies to electron and hole polarons and does not require any constraint on the wave functions during the self-consistent optimization. The implementation of this scheme does not produce any computational overhead compared to standard semilocal calculations and achieves fast convergence. This approach results in polaron properties, including the atomic geometry, the electron density, and the formation energy, which are close to those achieved with a hybrid functional that similarly satisfies the piece-wise linearity condition. This suggests that addressing the many-body self-interaction results in a polaron description that is robust with respect to the functional adopted. We illustrate our approach through applications to the electron polaron in $BiVO_4$, the hole polaron in MgO, and the hole trapped at the Al impurity in α-SiO_2.

DOI: 10.1103/PhysRevB.106.125119

I. INTRODUCTION

The polaron is a quasiparticle consisting of a localized charge dressed by its self-induced lattice distortions [1]. The occurrence of polaronic states affects the energetic and transport properties of electrons and holes, thereby arousing great interest in physics, chemistry, and material science [2–15]. Historically, the concept of polarons has been first discussed in 1933 by Landau [16], who introduced the idea of a trapped electron coupled with lattice distortions. In 1946, Pekar illustrated the first theoretical description of a free electron interacting with a polarizable dielectric continuum [17]. Subsequently, Landau and Pekar showed that such interactions can lead to the localization of the wave function, and to an increased effective mass [18]. This result inspired several studies based on effective Hamiltonians treating electron-phonon interactions. Depending on the strength of the electron-phonon interactions, two types of polarons are distinguished. In the limit of weak coupling, the polaron has a large spatial extension and is called large polaron (or Fröhlich polaron) [19]. At variance, in the limit of strong coupling, the polaron localizes over a short length scale comparable to the lattice parameter and is named small polaron (or Holstein polaron) [20]. Large polarons have generally been studied via Monte Carlo [21], path-integral Monte Carlo [22], and the renormalization group [23]. At variance, small polarons have mostly been investigated through first-principles approaches based on density functional theory (DFT) [24–33].

Density functional theory represents a powerful tool for modeling the atomic and electronic structures of real materials. However, semilocal DFT [34] generally fails in describing small polarons, because of its spurious inclusion of the electron self-interaction (SI). Indeed, the SI affects the polaron energetics and may oppose the electronic and structural localization of the polaron. Two types of SI have been distinguished [35–41]: the one-body and the many-body SI. The one-body SI generally refers to the way the interaction of a charge with itself is canceled in Hartree-Fock theory. At variance, the many-body SI corresponds to the deviation from the piece-wise linearity of the total energy upon electron occupation.

Many schemes have been developed to solve the problem of the one-body SI. In 1981, Perdew and Zunger proposed an approach that removes the single-particle SI pertaining to each electron state [42]. Subsequently, schemes that specifically address the one-body SI of the excess charge were proposed [43,44]. More recently, Sio *et al.* modeled electron-phonon interactions within an *ab initio* formulation and derived therefrom a one-body SI approach for polarons [45,46]. However, the cancellation of the one-body SI generally leads to very large polaron formation energies, on par with the overestimation of band gaps in Hartree-Fock theory [47].

Hybrid functionals offer a straightforward way to address the many-body SI. Early studies on polarons including exact exchange have been performed through the use of electronic structure codes employing atomic orbital basis set and

*stefano.falletta@epfl.ch

cluster models [48–53]. Subsequently, the use of exact exchange has been extended to account for periodic boundary conditions through developments in codes based on localized orbitals [54,55] and on plane waves [56–58]. In more recent studies addressing the many-body SI, the hybrid functional parameters are adjusted to enforce the piece-wise linearity of the total energy upon electron occupation [25,39,59]. Hybrid functionals satisfying such a constraint yield localized polarons [25,60–62] and band gaps in agreement with state-of-the-art *GW* calculations [25,59,63–66]. However, the use of hybrid functionals for modeling polarons demands computationally expensive structural and electronic relaxations as compared to semilocal functionals. This is particularly the case in plane-wave codes, but could represent a limiting factor also when using localized-orbital codes, for instance in molecular dynamics simulations.

At present, it remains unclear which of these two kinds of SI plays the dominant role in the physics of polarons [33,46,60]. Therefore, it is of interest to investigate the notions of one-body and many-body SI in a comparative fashion. Moreover, such a deeper analysis might provide insight into a route for modeling polarons free from SI at the semilocal level of theory. This would enable the study of polarons in large systems, in extended sets of materials, and in molecular dynamics evolving over long time periods.

In this paper, we investigate the concept of many-body self-interaction in relation to polarons in density functional theory. Our motivation is twofold. We aim to develop both (i) a comprehensive understanding of the relationship between one-body and many-body self-interaction and (ii) an efficient methodology for achieving charge localization at the semilocal level of theory. As case studies, we consider the electron polaron in $BiVO_4$, the hole polaron in MgO, and the trapped hole at the Al impurity in α-SiO_2. We begin our study on polarons by applying the piece-wise linearity condition to a hybrid functional and determining the respective electronic and structural properties, including the formation energy. To improve our conceptual understanding of the many-body self-interaction, we then focus on hybrid functionals containing a fraction α of Fock exchange, by which both forms of self-interaction can be covered. In this way, we find an analytical formulation for both the many-body and the one-body self-interaction and show that they are related through the dielectric constant. In particular, we demonstrate that these two forms of self-interaction coincide in the absence of electron screening. Next, taking advantage of the demonstrated preeminence of the many-body form of self-interaction, we develop a formulation at the semilocal level of theory for treating both electron and hole polarons. The localization is achieved by including a weak local potential in the semilocal Kohn-Sham Hamiltonian. This approach yields polarons with charge densities, atomic structures, and formation energies in close agreement with respect to the results obtained with the piece-wise linear hybrid functional but at the computational cost of a semilocal calculation. This result highlights the robustness of the electronic and structural properties of polarons free from many-body self-interaction. The present paper noticeably extends the contents of Ref. [47] in two directions. On the one hand, it contains the derivation of the unified formulation for the self-interaction with the role of the electron screening emphasized. On the other hand, it provides a more extensive account of the semilocal methodology for polaron localization with related applications.

The paper is organized as follows. In Sec. II, we study polarons as obtained with piece-wise linear hybrid functionals. In Sec. III A, we derive the unified theoretical framework for the concepts of one-body and many-body self-interaction. Section IV A is devoted to the development of the semilocal scheme for polaron localization and to its application to the case systems studied. In Sec. V, the conclusions are drawn.

II. POLARONS WITH HYBRID FUNCTIONALS

A. Semilocal functional

Without loss of generality, we here adopt a plane-wave-pseudopotential formulation. We take the Perdew-Burke-Ernzerhof (PBE) functional [34] as reference for our semilocal calculations. This consists in solving the following set of Kohn-Sham equations for each spin channel σ:

$$\mathcal{H}^0_\sigma[n^0_\uparrow, n^0_\downarrow]\psi^0_{i\sigma} = \epsilon^0_{i\sigma}\psi^0_{i\sigma}, \tag{1}$$

where $\mathcal{H}^0_\sigma$ is the PBE Hamiltonian, $\psi^0_{i\sigma}$ and $\epsilon^0_{i\sigma}$ are the resulting wave functions and energy levels, and $n^0_\sigma = \sum_i |\psi^0_{i\sigma}|^2$ is the electron density in the spin channel σ. The Hamiltonian $\mathcal{H}^0_\sigma$ is defined as

$$\mathcal{H}^0_\sigma[n^0_\uparrow, n^0_\downarrow] = -\tfrac{1}{2}\nabla^2 + V_{\rm ps} + V_{\rm H}[n^0] + V_{{\rm xc}\sigma}[n^0_\uparrow, n^0_\downarrow], \tag{2}$$

where $-\frac{1}{2}\nabla^2$ is the kinetic term, $V_{\rm ps}$ the sum of the local and nonlocal pseudopotentials, $V_{\rm H}$ the Hartree potential, $V_{{\rm xc}\sigma} = V_{{\rm x}\sigma} + V_{{\rm c}\sigma}$ the semilocal exchange-correlation potential, and $n^0 = \sum_\sigma n^0_\sigma$ the total electron density. We remark that the semilocal exchange potential $V_{{\rm x}\sigma}$ depends only on the density in the spin channel σ. This can be seen by using the exact relation [67]

$$V_{{\rm x}\sigma}[n^0_\uparrow, n^0_\downarrow] = V_{\rm x}[2n^0_\sigma], \tag{3}$$

where $V_{\rm x}[2n^0_\sigma]$ denotes the spin-unpolarized exchange potential evaluated for the density $2n^0_\sigma$. Then, the PBE energy is given by

$$E^0\big[\{\psi^0_{i\uparrow}\}, \{\psi^0_{i\downarrow}\}\big] = T[n^0] + E_{\rm H}[n^0] + E_{\rm xc}[n^0_\uparrow, n^0_\downarrow] + E_{\rm ps}\big[\{\psi^0_{i\uparrow}\}, \{\psi^0_{i\downarrow}\}\big] + E_{\rm Ewald}, \tag{4}$$

where T is the kinetic energy, $E_{\rm H}$ the Hartree energy, $E_{\rm xc} = E_{\rm x} + E_{\rm c}$ the semilocal exchange-correlation energy, $E_{\rm ps}$ the pseudopotential energy, and $E_{\rm Ewald}$ the Ewald energy.

B. Hybrid functional PBE0(α)

We consider the class of hybrid functionals PBE0(α) [68], in which a fraction α of Fock exchange is admixed to a fraction $(1-\alpha)$ of PBE local exchange. This corresponds to solving the following generalized Kohn-Sham equations:

$$\mathcal{H}^\alpha_\sigma\big[\{\psi^\alpha_{j\uparrow}\}, \{\psi^\alpha_{j\downarrow}\}\big]\psi^\alpha_{i\sigma} = \epsilon^\alpha_{i\sigma}\psi^\alpha_{i\sigma}, \tag{5}$$

where $\psi^\alpha_{i\sigma}$ and $\epsilon^\alpha_{i\sigma}$ are the resulting wave functions and energy levels, respectively, and the Hamiltonian $\mathcal{H}^\alpha_\sigma$ is given by

$$\mathcal{H}^\alpha_\sigma\big[\{\psi^\alpha_{i\uparrow}\}, \{\psi^\alpha_{i\downarrow}\}\big] = -\tfrac{1}{2}\nabla^2 + V_{\rm ps} + V_{\rm H}[n^\alpha] + V^\alpha_{{\rm xc}\sigma}[n^\alpha_\uparrow, n^\alpha_\downarrow] + V^\alpha_{\rm X}\big[\{\psi^\alpha_{i\sigma}\}\big], \tag{6}$$

where

$$V^{\alpha}_{\mathrm{xc}\sigma} = (1-\alpha)V_{\mathrm{x}\sigma} + V_{\mathrm{c}\sigma} \tag{7}$$

is the semilocal exchange-correlation potential,

$$V^{\alpha}_{\mathrm{X}}\left[\{\psi^{\alpha}_{i\sigma}\}\right](\mathbf{r},\mathbf{r}') = -\alpha\sum_i f_{i\sigma}\frac{\left|\psi^{\alpha}_{i\sigma}\right\rangle\left\langle\psi^{\alpha}_{i\sigma}\right|}{|\mathbf{r}-\mathbf{r}'|} \tag{8}$$

the Fock potential multiplied by α with $f_{i\sigma}$ being the electron occupation of the ith state in the spin channel σ, $n^{\alpha}_{\sigma} = \sum_i f_{i\sigma}|\psi^{\alpha}_{i\sigma}|^2$ the electron density in the spin channel σ, and $n^{\alpha} = \sum_{\sigma} n^{\alpha}_{\sigma}$ the total electron density. We remark that the Fock potential contributing to $\mathcal{H}^{\alpha}_{\sigma}$ is constructed using only the wave functions in the spin channel σ. Then, the PBE0(α) energy is given by

$$\begin{aligned} E^{\alpha}\left[\{\psi^{\alpha}_{i\uparrow}\},\{\psi^{\alpha}_{i\downarrow}\}\right] &= T[n^{\alpha}] + E_{\mathrm{H}}[n^{\alpha}] \\ &\quad + E^{\alpha}_{\mathrm{xc}}[n^{\alpha}_{\uparrow}, n^{\alpha}_{\downarrow}] + E^{\alpha}_{\mathrm{X}}\left[\{\psi^{\alpha}_{i\uparrow}\},\{\psi^{\alpha}_{i\downarrow}\}\right] \\ &\quad + E_{\mathrm{ps}}\left[\{\psi^{\alpha}_{i\uparrow}\},\{\psi^{\alpha}_{i\downarrow}\}\right] + E_{\mathrm{Ewald}}, \end{aligned} \tag{9}$$

where $E^{\alpha}_{\mathrm{xc}} = (1-\alpha)E_{\mathrm{x}} + E_{\mathrm{c}}$ is the semilocal exchange-correlation energy, and E^{α}_{X} the Fock energy. For $\alpha = 0$, PBE0(α) reduces to PBE.

Structural relaxations require the calculation of the atomic forces, which are defined as

$$F^{\alpha}_{I\mu} = -\frac{dE^{\alpha}}{d\boldsymbol{\tau}_{I\mu}}, \tag{10}$$

where $\boldsymbol{\tau}_{I\mu}$ denotes the Cartesian coordinate μ of the atom I. This is calculated through the Hellmann-Feynmann expression

$$F^{\alpha}_{I\mu} = -\left(\sum_{i\sigma}\left\langle\psi^{\alpha}_{i\sigma}\right|\frac{dV_{\mathrm{ps}}}{d\boldsymbol{\tau}_{I\mu}}\left|\psi^{\alpha}_{i\sigma}\right\rangle + \frac{dE_{\mathrm{Ewald}}}{d\boldsymbol{\tau}_{I\mu}}\right), \tag{11}$$

where the sum is carried out over all the occupied wave functions. When the wave functions $\psi^{\alpha}_{i\sigma}$ are expanded on a plane-wave basis set, no Pulay forces appear [69]. In Eq. (11), there are no explicit contributions resulting from electron-electron interactions (Hartree, exchange-correlation, Fock). Their influence on the atomic forces occurs via the self-consistent optimization of the wave functions $\psi^{\alpha}_{i\sigma}$.

C. Polaron formation energy

We consider a polaron of charge Q coupled with its self-induced lattice distortions $\mathbf{R}^{\alpha}_{Q}$, which are obtained by performing structural relaxation with PBE0(α). For electron polarons $Q = -1$, while for hole polarons $Q = +1$. Then, the PBE0(α) polaron formation energy is defined as [70,71]

$$E^{\alpha}_{\mathrm{f}}(Q) = E^{\alpha}(Q) - E^{\alpha}_{\mathrm{ref}}(0) + Q\epsilon^{\alpha}_{\mathrm{b}}, \tag{12}$$

where $E^{\alpha}(Q)$ is the total energy of the polaron system, $E^{\alpha}_{\mathrm{ref}}(0)$ the total energy of the pristine system, and $\epsilon^{\alpha}_{\mathrm{b}}$ the band edge corresponding to the delocalized state. The total energy $E^{\alpha}(Q)$ is related to the polaron level $\epsilon^{\alpha}_{\mathrm{p}}(Q)$ through Janak's theorem [72], namely,

$$\epsilon^{\alpha}_{\mathrm{p}}(Q) = -\left.\frac{dE^{\alpha}(q)}{dq}\right|_{q=Q}, \tag{13}$$

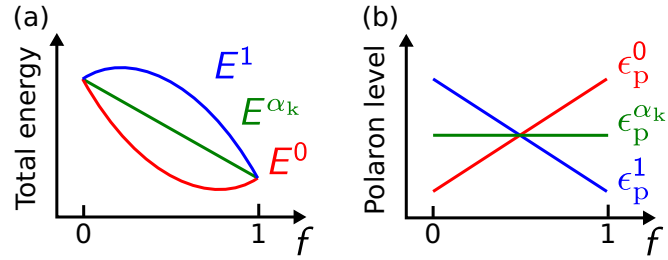

FIG. 1. Schematics of (a) the total energy E^{α} and of (b) the polaron level $\epsilon^{\alpha}_{\mathrm{p}}$ as a function of the electron occupation f of the polaron state for different PBE0(α) functionals.

where we have introduced the fractional polaron charge q to perform the derivative of the total energy with respect to charge at fixed geometry $\mathbf{R}^{\alpha}_{Q}$. The integral version of Eq. (13) reads

$$E^{\alpha}(Q) - E^{\alpha}(0) = -\int_0^Q dq\,\epsilon^{\alpha}_{\mathrm{p}}(q). \tag{14}$$

As illustrated in Fig. 1, the total energy $E^{\alpha}(q)$ generally shows either a positive or negative concavity with respect to the fractional polaron charge q. For $\alpha = 0$, PBE0(α) reduces to PBE, which is known to have a convex total energy as a function of q. On the other hand, for $\alpha = 1$, the nonlocal exchange operator in PBE0(α) is the same as in Hartree-Fock theory, which is characterized by a concave total energy as a function of q. For a specific value $\alpha = \alpha_{\mathrm{k}}$, PBE0($\alpha_{\mathrm{k}}$) is essentially piece-wise linear upon electron occupation and the polaron level is independent of q. In this case, the many-body SI vanishes.

In practice, the value α_{k} can be found by solving the following equation:

$$\left.\frac{d}{dq}\epsilon^{\alpha}_{\mathrm{p}}(q)\right|_{\alpha=\alpha_{\mathrm{k}}} = 0, \tag{15}$$

where α_{k} is found self-consistently with the geometry $\mathbf{R}^{\alpha}_{Q}$. Then, using Eq. (14), one can write

$$E^{\alpha_{\mathrm{k}}}(Q) = E^{\alpha_{\mathrm{k}}}(0) - Q\epsilon^{\alpha_{\mathrm{k}}}_{\mathrm{p}}. \tag{16}$$

By inserting Eq. (16) in Eq. (12) for $\alpha = \alpha_{\mathrm{k}}$, one obtains the following expression for the polaron formation energy:

$$E^{\alpha_{\mathrm{k}}}_{\mathrm{f}}(Q) = Q\left(\epsilon^{\alpha_{\mathrm{k}}}_{\mathrm{b}} - \epsilon^{\alpha_{\mathrm{k}}}_{\mathrm{p}}\right) + \left(E^{\alpha_{\mathrm{k}}}(0) - E^{\alpha_{\mathrm{k}}}_{\mathrm{ref}}(0)\right), \tag{17}$$

where the first and the second term on the right-hand side correspond to the energetic gain due to the electronic localization and to the energetic cost due to the lattice distortions, respectively.

D. Finite-size effects

The finite supercell size implies spurious interactions involving the polaron charge density due to the periodic boundary conditions [73–75]. As a consequence, the total energy and the polaron level are affected by finite-size effects, which need to be corrected. This can be done *a posteriori* via the scheme introduced by Falletta, Wiktor, and Pasquarello [75], which properly accounts for ionic polarization effects. We consider a system carrying a supercell charge q^* in which

the atomic positions have been relaxed in the presence of a supercell charge Q^*. For self-trapped polarons, the supercell charge q^* and Q^* coincide with the polaron charges q and Q, as in the cases of $BiVO_4$ and MgO. However, in the case of electrons and holes trapped at impurities, this relation does not generally apply. For instance, in the case of α-SiO_2, the hole trapping occurs in the neutral calculation ($q^* = Q^* = 0$), and the relations become $q^* = q - 1$ and $Q^* = Q - 1$.

The finite-size correction $E_{\rm cor}(q^*, \mathbf{R}_{Q^*})$ for the total energy pertaining to a system with supercell charge q^* in a geometry $\mathbf{R}_{Q^*}$ relaxed in the presence of a supercell charge Q^* is given by [75]

$$E_{\rm cor}(q^*, \mathbf{R}_{Q^*}) = E_{\rm m}(Q^*, \varepsilon_0) - E_{\rm m}(Q^* + Q^*_{\rm pol}, \varepsilon_\infty) + E_{\rm m}(q^* + Q^*_{\rm pol}, \varepsilon_\infty), \tag{18}$$

where $E_{\rm m}$ denotes the finite-size correction for regularly screened defects [73,74], ε_∞ and ε_0 are the high-frequency and static dielectric constants, respectively, and $Q^*_{\rm pol} = -Q^*(1 - \varepsilon_\infty/\varepsilon_0)$ is the ionic polarization charge associated to the polaron lattice distortions. The corresponding finite-size correction for the polaron level is obtained through Janak's theorem and is given by [75]

$$\epsilon_{\rm cor}(q^*, \mathbf{R}_{Q^*}) = -2\frac{E_{\rm m}(q^* + Q^*_{\rm pol}, \varepsilon_\infty)}{q^* + Q^*_{\rm pol}}. \tag{19}$$

To simplify the notation, the total energies and polaron levels throughout our paper are considered to be corrected by finite-size effects via the expressions in Eqs. (18) and (19).

The finite-size corrections depend on the high-frequency and static dielectric constants of the system under consideration. Through the application of finite electric fields [76], the dielectric tensor $\boldsymbol{\varepsilon}$ can be calculated as

$$\varepsilon_{ij} = 1 + \frac{4\pi}{\Omega}\frac{dp_i}{de_j}, \tag{20}$$

where Ω is the volume of the supercell, e_j the electric field along the direction j, and p_i the polarization in the direction i. For the evaluation of the high frequency dielectric tensor $\boldsymbol{\varepsilon}_\infty$, the structure is kept fixed, such that the polarization arises only from electronic relaxation. At variance, for the calculation of the static dielectric tensor $\boldsymbol{\varepsilon}_0$, the structure is relaxed in the presence of the electric field, to account for both the electronic and the ionic screening. In the case of anisotropic screening, the dielectric constant ε is obtained from the trace of $\boldsymbol{\varepsilon}$ as $\varepsilon = {\rm Tr}(\boldsymbol{\varepsilon})/3$.

E. Case studies and computational details

The calculations are performed using a plane-wave density functional approach as implemented in the QUANTUM ESPRESSO suite [57]. We use the semilocal functional PBE [34] and the hybrid functional PBE0(α) [68]. The core-valence interactions are described by normconserving pseudopotentials [77]. As case studies, we consider the electron polaron in $BiVO_4$ [26], the hole polaron in MgO [24], and the hole trapped at the Al impurity in α-SiO_2 [24,43,51,52,78,79]. We model $BiVO_4$ with a 96-atom orthorhombic supercell ($a = 10.34$ Å, $b = 10.34$ Å, $c = 11.79$ Å), MgO with a 64-atom cubic supercell ($a = 8.45$ Å), and α-SiO_2 with a 72-atom hexagonal supercell ($a = 9.97$ Å, $c = 10.96$ Å). The lattice parameters and the atomic positions are optimized at the semilocal level of theory for the pristine systems. We sample the Brillouin zone at Γ point and set the energy cutoff to 100 Ry in all cases. The electron and hole polarons are obtained by either adding or removing one electron from the system. In the case of α-SiO_2, a hole is trapped at the Al site in the neutral system. The polaron structures are obtained through atomic relaxation at fixed supercell parameters.

TABLE I. High-frequency and static dielectric constants, ε_∞ and ε_0, respectively, for the systems considered in this paper, as calculated with the functional PBE.

System	ε_∞	ε_0
$BiVO_4$	5.83	64.95
MgO	2.77	10.73
α-SiO_2	2.25	4.52

The high-frequency and static dielectric tensors, $\boldsymbol{\varepsilon}_\infty$ and $\boldsymbol{\varepsilon}_0$, respectively, are determined by applying finite electric fields [76] at the semilocal level of theory. We use the values $e_j = 0, 1 \times 10^{-4}, 2.5 \times 10^{-4}, 5 \times 10^{-4}$ a.u. ($j = x, y, z$) and perform a linear regression to find the components of the dielectric tensors. In the case of isotropic screening (MgO), the electric field is applied only along one Cartesian direction. At variance, in the case of anisotropic screening ($BiVO_4$, α-SiO_2), the electric field is applied along the three Cartesian directions. The obtained values of the dielectric constants are given in Table I and are used for the determination of the finite-size effects [75]. The finite-size corrections for total energies and polaron levels are given in Table II. In the case of α-SiO_2, the hole trapping occurs in a neutral calculation and is not affected by finite-size effects.

F. Hybrid-functional results

In Fig. 2, we show the polaron density obtained with PBE0($\alpha_{\rm k}$) for all cases studied. In $BiVO_4$, the electron polaron localizes on a vanadium atom, thereby causing an elongation of the neighboring V-O bonds from 1.73 to 1.80 Å. In MgO, the hole polaron is centered on an oxygen atom, thereby elongating the neighboring Mg-O bonds from 2.11 to 2.20 Å. In α-SiO_2, the hole is trapped at the Al impurity, with three short Al-O bonds of 1.69 Å and one long Al-O bond of 1.91 Å.

For each system, the fraction $\alpha_{\rm k}$ of Fock exchange used in the polaron calculation is determined according to Eq. (15) as

TABLE II. Finite-size corrections of total energies and polaron levels for the systems with and without polaron charge in the polaron geometry. All values are in eV.

	With polaron		Without polaron	
System	$E_{\rm cor}$	$\epsilon_{\rm cor}$	$E_{\rm cor}$	$\epsilon_{\rm cor}$
$BiVO_4$	0.03	0.06	0.29	−0.58
MgO	0.13	−0.25	0.59	1.34
α-SiO_2	0.00	0.00	1.24	2.47

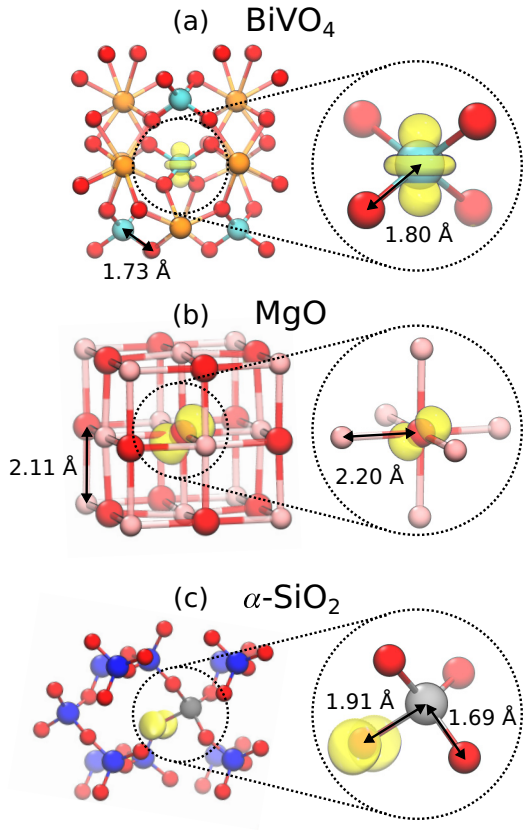

FIG. 2. Polaron isodensity surface at 5% of its maximum calculated with PBE0(α_k) for the electron polaron in $BiVO_4$, the hole polaron in MgO, and the hole trapped at the Al impurity in α-SiO_2 (Bi in orange, V in cyan, O in red, Mg in pink, Si in blue, Al in grey).

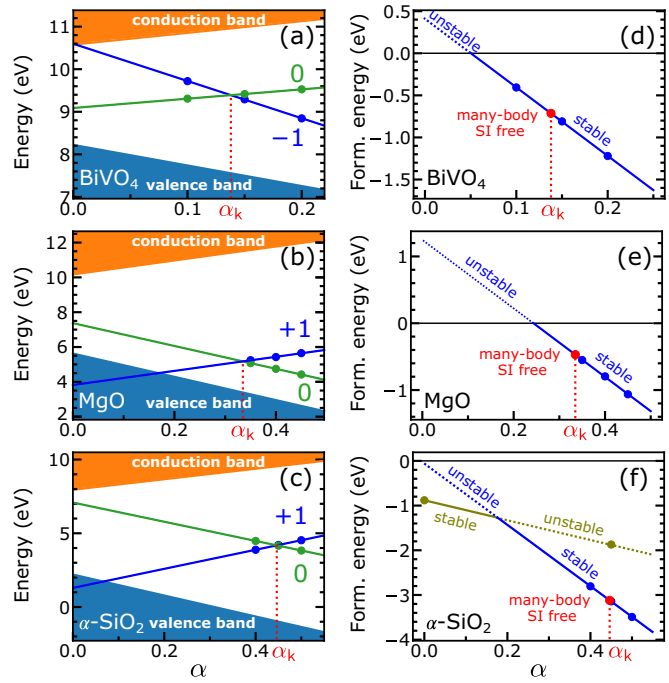

FIG. 3. [(a)–(c)] Energy levels and [(d)–(f)] formation energies obtained with PBE0(α) as a function α for the electron polaron in $BiVO_4$, the hole polaron in MgO, and the hole trapped at the Al impurity in α-SiO_2. The polaron levels are identified by their respective polaron charge. In all cases, the polaron geometry is obtained with PBE0(α_k).

follows. We first fix an approximate value of α_k and relax the polaron to find the geometry $\mathbf{R}_Q^{\alpha_k}$. Second, for this geometry, we obtain the levels $\epsilon_p^\alpha(0)$ and $\epsilon_p^\alpha(Q)$ pertaining to the charge states 0 and Q as a function of α. Their intersection gives an improved value for α_k, with which the procedure is repeated until self-consistency is reached. As illustrated in Figs. 3(a)–3(c), we find $\alpha_k = 0.14$, 0.34, and 0.l145 for $BiVO_4$, MgO, and α-SiO_2, respectively. This study allows us to determine the polaron level $\epsilon_p^{\alpha_k}$.

From $\epsilon_p^{\alpha_k}$, we obtain the formation energies via Eq. (17) for all the systems under consideration. For $BiVO_4$, MgO, and α-SiO_2, we find −0.63 eV, −0.53 eV, and −3.11 eV, respectively. In the case of α-SiO_2, the larger formation energy stems from the fact that the hole is not self-trapped but bound to the Al impurity. Furthermore, we illustrate in Figs. 3(d)–3(f) the polaron stability as a function of the fraction of Fock exchange α using the formation energy of Eq. (12) at fixed geometry $\mathbf{R}_Q^{\alpha_k}$. The PBE0(α) formation energies are found to be very sensitive to α, which is an effect mainly resulting from the strong dependence of the band edge ϵ_b^α on α [cf. Figs. 3(a)–3(c)]. Moreover, the polaron at $\alpha = 0$ (i.e., PBE) is not stable in all cases. This emphasizes that the functional PBE fails in localizing the polaronic states. In the case of α-SiO_2, we also calculate the formation energy corresponding to the geometry found in PBE, in which the hole is delocalized over the four nearest neighbor O atoms (Al-O bond lengths of 1.74 Å). Also in this case, the hole trapped at a single O atom is unstable at $\alpha = 0$, in accord with previous studies [51,52]. At variance, for $\alpha = \alpha_k$, the one-site polaron is found to be more stable than the four-site polaron by 1.25 eV.

To assess the overall quality of the electronic structure, it is of interest to compare the PBE0(α_k) band gaps with experimental values. The comparison with experiment requires the consideration of relevant effects, such as due to spin-orbit coupling, atomic vibrations (zero-point phonon renormalization), electron-hole interaction (for optical band gaps), and magnetic ordering [80,89,90]. For PBE0(α) functionals, the agreement with experiment is generally rather good when such effects are accounted for [25,59,63,64,66,91–93]. In particular, for $BiVO_4$, MgO, and α-SiO_2, we indeed find errors of at most 0.25 eV when comparing PBE0(α_k) band gaps with relevant experimental values after including suitable corrections (see Table III), consistent with typical values for the mean absolute errors in such comparisons [25,66].

We remark that the enforcement of the piece-wise linearity condition is in principle defect dependent. As investigated in Refs. [25,63–65], α_k can vary up to ±0.03 depending on the defect under consideration. However, by selecting an optimal defect ensuring minimal hybridization with the delocalized band states, the uncertainty in α_k can be further reduced [64]. Accurate comparisons with experimental band gaps in Refs. [64,66] show agreement within 0.25 eV. The dependence of α_k on the defect considered ultimately reflects the approximate nature of the PBE0(α) functional.

TABLE III. Band gaps calculated with PBE (E_g^0) and PBE0(α_k) ($E_g^{\alpha_k}$) compared to experimental values after including suitable corrections (ΔE_g). Energies are in eV.

	E_g^0	$E_g^{\alpha_k}$	ΔE_g	$E_g^{\alpha_k}+\Delta E_g$	Expt.
$BiVO_4$	2.38	3.41	−1.16[a]	2.25	2.4–2.5[b]
MgO	4.65	8.15	−0.53[c]	7.62	7.77[d]
α-SiO_2	5.81	10.51	0.02[d]	10.53	10.30[f]

[a]Reference [80], including spin-orbit coupling, thermal vibrations, and exciton binding energy.
[b]References [81–83], optical band gap at 300 K.
[c]Reference [84], zero-point phonon renormalization.
[d]Reference [85], fundamental band gap at 6 K.
[e]Separation of 0.60 eV between fundamental band gap and first absorption peak [86], and zero-point phonon renormalization of −0.58 eV [87].
[f]Reference [88], first peak in reflectance spectrum.

III. UNIFIED FORMULATION FOR THE SELF-INTERACTION

A. Many-body self-interaction

In this section, we consider a localized polaron with the atomic structure $\mathbf{R}_Q^{\alpha_k}$. The single-particle levels are known to depend linearly on α in PBE0(α) calculations [25,28,33,59,63,64]. Furthermore, the total energy $E^\alpha(q)$ obtained with PBE0(α) generally shows a quadratic behavior upon fractional charge addition [7,40]. Hence, through Janak's theorem [72],

$$\epsilon_p^\alpha(q) = -\frac{dE^\alpha(q)}{dq}, \tag{21}$$

the polaron level $\epsilon_p^\alpha(q)$ can be taken to depend linearly on both q and α. As demonstrated in Appendix A, these assumptions imply that the variations of the polaron wave function with q, the second-order derivative of the wave functions of the valence states with respect to q, and the variations of the wave functions with α can be taken to vanish. We denote ψ_p the wave function of the polaron state and $n_p = |\psi_p|^2$ the polaron density. The electron (hole) polaron state is identified as the last-occupied (first unoccupied) state.

We then expand $\epsilon_p^\alpha(q)$ in α around α_k,

$$\epsilon_p^\alpha(q) = \epsilon_p^{\alpha_k} + (\alpha-\alpha_k)\frac{d\epsilon_p^\alpha(q)}{d\alpha}, \tag{22}$$

where $\epsilon_p^{\alpha_k}$ is independent of q because of the definition of α_k [cf. Eq. (15)]. By further expanding the right-hand side of Eq. (22) with respect to q around $q=0$, we get

$$\epsilon_p^\alpha(q) = \epsilon_p^{\alpha_k} + (\alpha-\alpha_k)\left[\frac{d\epsilon_p^\alpha(0)}{d\alpha} + q\frac{d^2\epsilon_p^\alpha(q)}{d\alpha dq}\right]. \tag{23}$$

By introducing the fractional charge q_k defined as

$$q_k = -\frac{d\epsilon_p^\alpha(0)}{d\alpha}\Big/\frac{d^2\epsilon_p^\alpha(q)}{d\alpha dq}, \tag{24}$$

we can rewrite Eq. (23) as

$$\epsilon_p^\alpha(q) = \epsilon_p^{\alpha_k} + (\alpha-\alpha_k)(q-q_k)\frac{d^2\epsilon_p^\alpha(q)}{d\alpha dq}. \tag{25}$$

The result in Eq. (25) can be equivalently obtained by first expanding $\epsilon_p^\alpha(q)$ in q around q_k and then by expanding in α around α_k. In this case, we get the following expression for α_k:

$$\alpha_k = -\frac{d\epsilon_p^0(q)}{dq}\Big/\frac{d^2\epsilon_p^\alpha(q)}{d\alpha dq}, \tag{26}$$

which is analogous to Eq. (24). By taking the ratio between the expressions in Eqs. (24) and (26), we find a relationship that links α_k and q_k,

$$\frac{q_k}{\alpha_k} = \frac{d\epsilon_p^\alpha(0)}{d\alpha}\Big/\frac{d\epsilon_p^0(q)}{dq}, \tag{27}$$

which emphasizes the duality between α_k and q_k in the expression of $\epsilon_p^\alpha(q)$ [cf. Eq. (25)].

We define the many-body SI energy correction to the PBE0(α) energy as

$$\Delta E^\alpha(q)|_{mb} = \left[E^\alpha(0) - q\epsilon_p^{\alpha_k}\right] - E^\alpha(q), \tag{28}$$

such that the energy $E^\alpha(q) + \Delta E^\alpha(q)|_{mb}$ is piece-wise linear as a function of q. At $\alpha=\alpha_k$, $\Delta E^{\alpha_k}|_{mb}$ vanishes by definition of α_k. The total energy $E^\alpha(q)$ in Eq. (28) can be expanded at second order in q as

$$E^\alpha(q) - E^\alpha(0) = -q\epsilon_p^\alpha(0) - \frac{q^2}{2}\frac{d\epsilon_p^\alpha(q)}{dq}, \tag{29}$$

where we have applied Janak's theorem [Eq. (21)] for expressing the first and the second derivative of the total energy with respect to q in terms of the polaron level. By inserting Eq. (29) in Eq. (28) and by expressing $\epsilon_p^{\alpha_k} = \epsilon_p^\alpha(q_k)$, we get

$$\Delta E^\alpha(q)|_{mb} = q\left[\epsilon_p^\alpha(0) - \epsilon_p^\alpha(q_k)\right] + \frac{q^2}{2}\frac{d\epsilon_p^\alpha(q)}{dq}. \tag{30}$$

By using the linearity of the polaron level in q, the latter equation becomes

$$\Delta E^\alpha(q)|_{mb} = \frac{1}{2}[(q-q_k)^2 - q_k^2]\frac{d\epsilon_p^\alpha(q)}{dq}. \tag{31}$$

Expanding $\epsilon_p^\alpha(q)$ in α and using the definition of α_k in Eq. (26), we obtain

$$\frac{d\epsilon_p^\alpha(q)}{dq} = \left(1-\frac{\alpha}{\alpha_k}\right)\frac{d\epsilon_p^0(q)}{dq} = -\left(1-\frac{\alpha}{\alpha_k}\right)\frac{d^2E^0(q)}{dq^2}, \tag{32}$$

where the second equality stems from Janak's theorem. This allows us to express Eq. (31) as

$$\Delta E^\alpha(q)|_{mb} = -\frac{1}{2}\left(1-\frac{\alpha}{\alpha_k}\right)[(q-q_k)^2 - q_k^2]\frac{d^2E^0(q)}{dq^2}. \tag{33}$$

Using the chain rule on the second derivative of the total energy with respect to q, we get

$$\Delta E^{\alpha}(q)|_{\rm mb} = -\left(1-\frac{\alpha}{\alpha_{\rm k}}\right)[(q-q_{\rm k})^2 - q_{\rm k}^2]\left\{E_{\rm H}\left[\frac{dn}{dq}\right] + \frac{1}{2}\sum_{\sigma\sigma'}\int d\mathbf{r}d\mathbf{r}'\,\frac{\delta^2 E_{\rm xc}[n_\uparrow, n_\downarrow]}{\delta n_\sigma(\mathbf{r})\delta n_{\sigma'}(\mathbf{r}')}\frac{dn_\sigma(\mathbf{r})}{dq}\frac{dn_{\sigma'}(\mathbf{r})}{dq}\right\}, \tag{34}$$

where the second derivatives of n_σ with respect to q have been taken to vanish and the superscript 0 in the densities n_σ has been skipped, consistently with the assumptions of our formulation (see Appendix A). In Eq. (34), the Fock exchange effects are entirely described by $q_{\rm k}$ and $\alpha_{\rm k}$. Apart from the parameters $q_{\rm k}$ and $\alpha_{\rm k}$, $\Delta E^{\alpha}|_{\rm mb}$ is herewith expressed in terms of a quantity that can be evaluated at the semilocal PBE level. By applying Janak's theorem to $\Delta E^{\alpha}(q)|_{\rm mb}$ in Eq. (33), we find the many-body SI correction to the polaron level

$$\begin{aligned}\Delta\epsilon_{\rm p}^{\alpha}(q)\big|_{\rm mb} &= -\frac{d}{dq}\Delta E^{\alpha}(q)|_{\rm mb} \\ &= -\left(1-\frac{\alpha}{\alpha_{\rm k}}\right)(q-q_{\rm k})\frac{d\epsilon_{\rm p}^{0}(q)}{dq},\end{aligned} \tag{35}$$

which vanishes at both $\alpha = \alpha_{\rm k}$ or $q = q_{\rm k}$, consistently with Eq. (25). Thus, the polaron level $\epsilon_{\rm p}^{\alpha} + \Delta\epsilon_{\rm p}^{\alpha}|_{\rm mb}$ is constant for varying polaron charge q. Applying the Hellmann-Feynman theorem to the derivative of $\epsilon_{\rm p}^{0}(q)$ with respect to q, we get

$$\frac{d\epsilon_{\rm p}^{0}(q)}{dq} = \langle\psi_{\rm p}|\frac{d\mathcal{H}_{\sigma_{\rm p}}^{0}(q)}{dq}|\psi_{\rm p}\rangle\,. \tag{36}$$

Then, using the chain rule on the derivative of the Hamiltonian $\mathcal{H}_{\sigma_{\rm p}}^{0}(q)$ with respect to q, Eq. (35) can be rewritten as

$$\begin{aligned}\Delta\epsilon_{\rm p}^{\alpha}(q)\big|_{\rm mb} = -\left(1-\frac{\alpha}{\alpha_{\rm k}}\right)(q-q_{\rm k})\int d\mathbf{r}\left\{V_{\rm H}\left[\frac{dn}{dq}\right](\mathbf{r})\right. \\ \left. + \sum_{\sigma}\int d\mathbf{r}'\,\frac{\delta V_{{\rm xc}\sigma_{\rm p}}[n_\uparrow, n_\downarrow](\mathbf{r})}{\delta n_\sigma(\mathbf{r}')}\frac{dn_\sigma(\mathbf{r}')}{dq}\right\}n_{\rm p}(\mathbf{r}),\end{aligned} \tag{37}$$

where $\sigma_{\rm p}$ is the spin channel corresponding to the polaron state.

We evaluate the many-body SI corrected total energy and polaron level as a function of q for the cases studied. Here, we determine the polaron energetics at $\alpha = 0$ (PBE) at first-order perturbation theory using the wave functions and the atomic structure obtained with the hybrid functional PBE0($\alpha_{\rm k}$). The many-body SI corrections are evaluated using the following finite-difference expression for $d\epsilon_{\rm p}^{0}(q)/dq$:

$$\frac{d\epsilon_{\rm p}^{0}(q)}{dq} = \frac{\epsilon_{\rm p}^{0}(Q) - \epsilon_{\rm p}^{0}(0)}{Q}, \tag{38}$$

where the levels $\epsilon_{\rm p}^{0}(Q)$ and $\epsilon_{\rm p}^{0}(0)$ are calculated with the functional PBE. As illustrated in Figs. 4(a)–4(b) in the cases of $BiVO_4$ and α-SiO_2, the PBE total energy exhibits a concavity upon partial electron occupation, and a corresponding linear variation of the polaron level [cf. Figs. 4(c) and 4(d)]. Upon applying the corrections $\Delta E^{0}(q)|_{\rm mb}$ and $\Delta\epsilon_{\rm p}^{0}(q)|_{\rm mb}$, the total energy and the polaron level become linear and constant in q, respectively.

The electron screening affects the many-body SI corrections in Eqs. (34) and (37) through the derivatives dn_σ/dq. To illustrate such screening effects, it is convenient to focus on the density of valence electrons. Covering the cases of both electron and hole polarons, this can be expressed as

$$n_{\sigma\,\rm val}(q) = n_\sigma(q) + \delta_{\sigma,\sigma_{\rm p}}qn_{\rm p}, \tag{39}$$

where δ is the Kronecker delta. Then, the variations of $n_{\sigma\,\rm val}(q)$ with respect to q can be calculated by finite differences as

$$\frac{dn_{\sigma\,\rm val}(q)}{dq} = \frac{n_\sigma(Q) + \delta_{\sigma,\sigma_{\rm p}}Qn_{\rm p} - n_\sigma(0)}{Q}. \tag{40}$$

These variations are shown in Fig. 5 for both spin channels in the cases of the electron polaron in $BiVO_4$ and the hole trapped at the Al impurity in α-SiO_2. First, we remark that the response of the valence electrons with respect to the polaron charge is not negligible compared to the polaron charge density. Second, the screening effects in the two spin channels are noticeably different. This emphasizes the limitation of using the restricted open-shell Kohn-Sham (ROKS) constraint in the self-consistent optimization of the Kohn-Sham equations.

B. One-body self-interaction

We define the one-body SI energy correction to $E^{\alpha}(q)$ as

$$\Delta E^{\alpha}(q)|_{\rm ob} = \left[E^{1}(q) - E^{1}(0)\right] - \left[E^{\alpha}(q) - E^{\alpha}(0)\right], \tag{41}$$

which reproduces the q dependence of the energy found for the Hartree-Fock like regime at $\alpha = 1$. The correction $\Delta E^{\alpha}(q)|_{\rm ob}$ vanishes for $\alpha = 1$. Given the linearity of the total

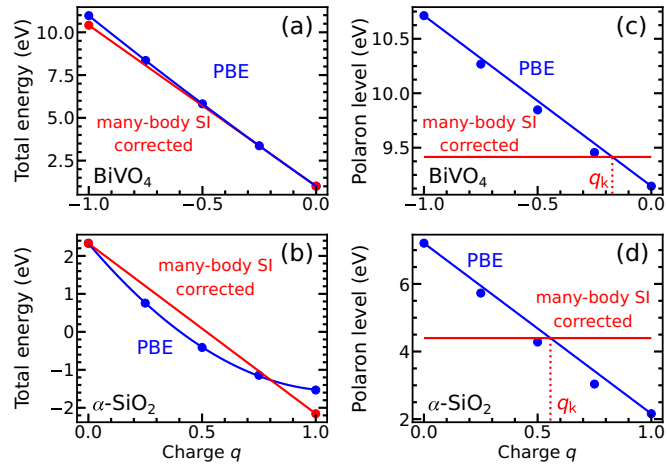

FIG. 4. Many-body self-interaction corrected [(a),(b)] total energy $E^{0}(q)$ and [(c),(d)] polaron level $\epsilon_{\rm p}^{0}(q)$ as a function of the charge q, for the electron polaron in $BiVO_4$ and for the trapped hole at the Al impurity in α-SiO_2. The localized polarons are obtained with the hybrid functional PBE0($\alpha_{\rm k}$). The results for MgO are shown in Ref. [47].

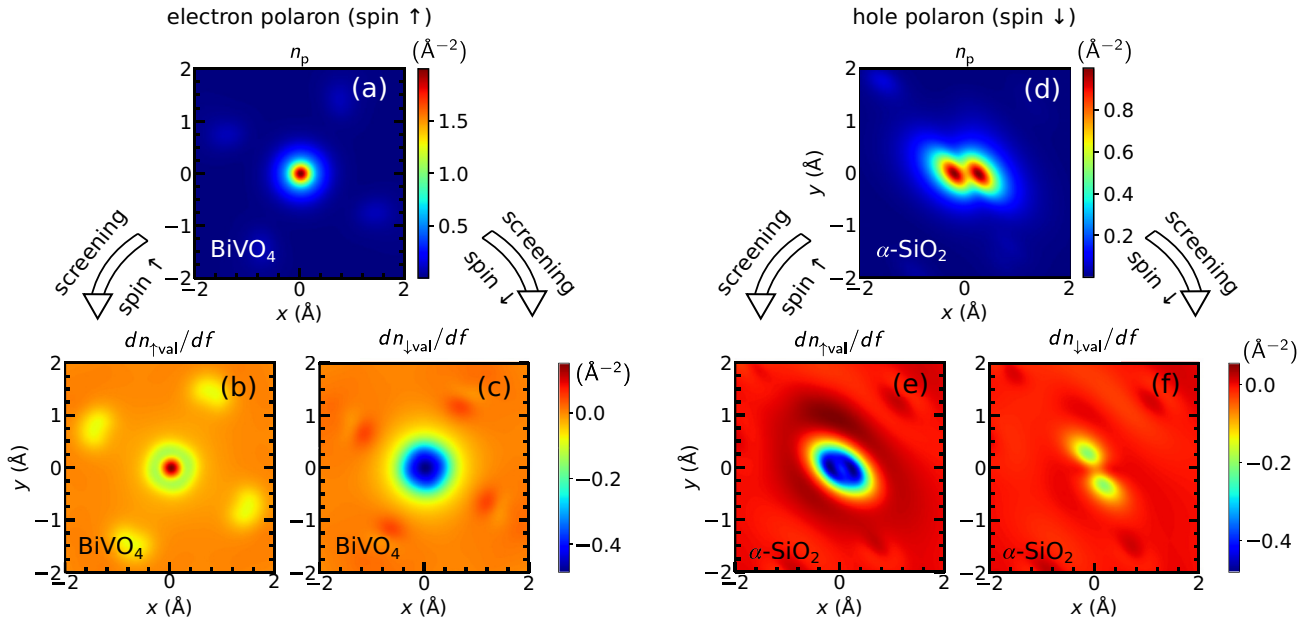

FIG. 5. [(a), (d)] Polaron density n_p and [(b), (c), (e), (f)] variation of the valence-electron densities $n_{\sigma val}$ upon the occupation f of the polaron level [cf. Eq. (40)] for the electron polaron in $BiVO_4$, and the hole polaron in α-SiO_2, as obtained with the functional PBE0(α_k). The densities are integrated over the z direction and plotted in the xy plane. The results for the hole polaron in MgO are shown in Ref. [47].

energy with respect to α, Eq. (41) can be rewritten as

$$\Delta E^{\alpha}(q)|_{ob} = (1-\alpha)\frac{d}{d\alpha}[E^{\alpha}(q) - E^{\alpha}(0)]. \quad (42)$$

Using the total energy expansion in Eq. (29), the definitions of q_k and α_k in Eqs. (24) and (26), and Janak's theorem in Eq. (21), we find

$$\Delta E^{\alpha}(q)|_{ob} = -\frac{1}{2}\frac{(1-\alpha)}{\alpha_k}[(q-q_k)^2 - q_k^2]\frac{d^2E^0(q)}{dq^2}. \quad (43)$$

Using Janak's theorem, the one-body energy correction to the polaron level is obtained as

$$\begin{aligned}\Delta\epsilon_p^{\alpha}(q)\big|_{ob} &= -\frac{d}{dq}\Delta E^{\alpha}(q)|_{ob} \\ &= -(q-q_k)\frac{(1-\alpha)}{\alpha_k}\frac{d\epsilon_p^0(q)}{dq}, \end{aligned} \quad (44)$$

which corresponds to the energy difference $\epsilon_p^1(q) - \epsilon_p^{\alpha}(q)$. Interestingly, the one-body SI energy corrections can be derived starting from the many-body SI energy corrections. For the total energy, one has

$$\Delta E^{\alpha}(q)|_{ob} = \Delta E^{\alpha}(q)|_{mb} - \Delta E^{1}(q)\big|_{mb}. \quad (45)$$

Similarly, for the polaron level,

$$\Delta\epsilon_p^{\alpha}(q)\big|_{ob} = \Delta\epsilon_p^{\alpha}(q)\big|_{mb} - \Delta\epsilon_p^{1}(q)\big|_{mb}. \quad (46)$$

This relation is illustrated in Fig. 6 in the case of a hole polaron.

The relationship between the two forms of SI can be further highlighted by taking the ratio between $\Delta E^{\alpha}(q)|_{mb}$ and $\Delta E^{\alpha}(q)|_{ob}$ in Eqs. (33) and (43),

$$\Delta E^{\alpha}(q)|_{mb} = \frac{\alpha_k - \alpha}{1-\alpha}\Delta E^{\alpha}(q)|_{ob}, \quad (47)$$

which reveals that these two forms of SI are related by a proportionality relation. For $\alpha = 0$ (PBE), Eq. (47) takes the simple form

$$\Delta E^{0}(q)|_{mb} = \alpha_k \Delta E^{0}(q)|_{ob}. \quad (48)$$

The parameter α_k is generally related to electron screening, as represented by the high-frequency dielectric constant ε_∞ [94,95]. In particular, $\alpha_k \simeq 1/\varepsilon_\infty$ reproduces the correct asymptotic potential in the long-range limit [39,96]. Additionally, this choice of α generally yields band gaps in good agreement with experiment [25,63,97,98] upon proper consideration of renormalization due to thermal vibrations, spin-orbit coupling, and excitonic and magnetic ordering effects [80,89,90]. Hence, Eq. (48) can be rewritten as

$$\Delta E^{0}(q)|_{mb} \simeq \frac{1}{\varepsilon_\infty}\Delta E^{0}(q)|_{ob}, \quad (49)$$

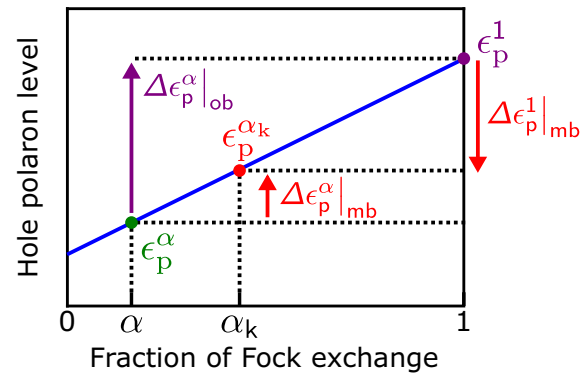

FIG. 6. One-body and many-body SI energy correction for a hole polaron level $\epsilon_p^{\alpha}(Q=+1)$, illustrating Eq. (46).

TABLE IV. Screening effects in electron density and Coulomb kernel for the various forms of self-interaction.

Screening	Many-body	One-body	Bare
Electron density	√	√	✗
Coulomb kernel	√	✗	✗

which establishes a quantitative relationship between these SI energies in case of $\alpha = 0$. Equation (49) carries similarity with the Hartree-Fock theory of excitons [99,100]. Indeed, when calculating the exciton binding energy, the bare Coulomb kernel $1/|\mathbf{r} - \mathbf{r}'|$ is replaced with the screened kernel $1/(\epsilon_\infty|\mathbf{r} - \mathbf{r}'|)$, which includes the dielectric constant analogously to Eq. (49). Hence, the account of screening effects in the many-body SI emphasizes its superiority over the one-body SI.

The connection between many-body and one-body forms of SI can be further highlighted by turning off the electron screening. This can be achieved by setting equal to zero the variations of the wave functions with respect to q. Starting from Eq. (39), this gives

$$\left.\frac{dn_\sigma}{dq}\right|_{\text{bare}} = -\delta_{\sigma,\sigma_\text{p}} n_\text{p}. \tag{50}$$

In this limit, we apply the Hellmann-Feynmann theorem to $d\epsilon^\alpha_\text{p}(q)/dq$ and obtain

$$\left.\frac{d\epsilon^\alpha_\text{p}(q)}{dq}\right|_{\text{bare}} = \langle\psi_\text{p}| \left.\frac{d\mathcal{H}^\alpha_{\sigma_\text{p}}(q)}{dq}\right|_{\text{bare}} |\psi_\text{p}\rangle\,. \tag{51}$$

Using the chain rule similarly to Eq. (37), neglecting the variations of the valence wave functions with q, and noticing that

$$\langle\psi_\text{p}| \frac{|\psi_\text{p}\rangle\langle\psi_\text{p}|}{|\mathbf{r} - \mathbf{r}'|} |\psi_\text{p}\rangle = \langle\psi_\text{p}|V_\text{H}[n_\text{p}]|\psi_\text{p}\rangle\,, \tag{52}$$

we get

$$\left.\frac{d\epsilon^\alpha_\text{p}(q)}{dq}\right|_{\text{bare}} = -\langle\psi_\text{p}| \left\{(1-\alpha)V_\text{H}[n_\text{p}] + \int d\mathbf{r}\, \frac{\delta V^\alpha_{\text{xc}\sigma_\text{p}}[n_\uparrow, n_\downarrow]}{\delta n_{\sigma_\text{p}}(\mathbf{r})} n_\text{p}(\mathbf{r})\right\} |\psi_\text{p}\rangle\,. \tag{53}$$

Considering that $V^\alpha_{\text{xc}\sigma_\text{p}} = (1-\alpha)V_{\text{x}\sigma_\text{p}} + V_{\text{c}\sigma_\text{p}}$ [cf. Eq. (7)], one finds that the right hand side of Eq. (53) vanishes for $\alpha = 1$, apart from weaker correlation terms. Hence, the piece-wise linearity condition of Eq. (15) is satisfied for $\alpha^\text{bare}_\text{k} = 1$. In the limit in which the electron screening is turned off, the many-body and one-body forms of SI coincide and are equal to

$$\Delta E^\alpha(q)|_{\text{bare}} = -(1-\alpha)[(q - q^\text{bare}_\text{k})^2 - (q^\text{bare}_\text{k})^2] \cdot \left\{E_\text{H}[n_\text{p}] + \frac{1}{2}\int d\mathbf{r}d\mathbf{r}'\, \frac{\delta^2 E_\text{xc}[n_\uparrow, n_\downarrow]}{\delta n_{\sigma_\text{p}}(\mathbf{r})\delta n_{\sigma_\text{p}}(\mathbf{r}')} n_\text{p}(\mathbf{r}) n_\text{p}(\mathbf{r}')\right\}. \tag{54}$$

A summary of the screening effects in the density and Coulomb kernel for the various forms of SI studied in this paper is given in Table IV.

TABLE V. Polaron binding energies corrected for different forms of self-interaction. For self-trapped polarons, the binding energy coincides with the formation energy in absolute value. In the case of α-SiO_2, the binding energy measures the stability of the hole localized at one O atom with respect to the hole delocalized over four O atoms. The binding energies free from many-body and one-body SI are obtained with PBE0(α_k) and PBE0($\alpha = 1$), respectively. The binding energy including the SI correction proposed by Sio *et al.* is obtained through Eq. (58).

System	Many-body SI	One-body SI	SI of Sio *et al.*
$BiVO_4$	0.63	7.73	3.34
MgO	0.53	3.88	1.98
α-SiO_2	1.25	3.83	1.56

It is interesting to note that the expression in Eq. (54) evaluated at $\alpha = 0$ essentially coincides with the SI energy correction found by Sio *et al.* [45,46],

$$\Delta E^0(q)\big|_{\text{Sio}} = -q^2 \left\{E_\text{H}[n_\text{p}] + \frac{1}{2}\int d\mathbf{r}d\mathbf{r}'\, \frac{\delta^2 E_\text{xc}[n_\uparrow, n_\downarrow]}{\delta n_{\sigma_\text{p}}(\mathbf{r})\delta n_{\sigma_\text{p}}(\mathbf{r}')} n_\text{p}(\mathbf{r}) n_\text{p}(\mathbf{r}')\right\}. \tag{55}$$

Indeed, in their derivation, Sio *et al.* neglected the electron screening effects like in our bare approximation. The only difference between the two expressions arises from the q-dependent prefactor, which is related to the different definitions adopted for the SI-corrected energy functional. In our case [cf. Eq. (28)],

$$E^0(q)\big|_{\text{bare}} + \Delta E^0(q)\big|_{\text{bare}} = E^0(0) - q\,\epsilon^0_\text{p}\big(q^\text{bare}_\text{k}\big)\big|_{\text{bare}}, \tag{56}$$

whereas, in the case of Sio *et al.*, the total energy $E^0(q)$ is expanded in q around $q = 0$ and the second-order derivative of $E^0(q)$ with respect to q is removed. This results in

$$E^0(q)|_{\text{bare}} + \Delta E^0(q)|_{\text{Sio}} = E^0(0) - q\epsilon^0_\text{p}(0). \tag{57}$$

Hence, in the absence of electron screening, the difference between our bare expression and that derived in Refs. [45,46] can be associated with the slope of the linear dependence of SI corrected energy functional with q, which corresponds to the polaron level at $q = 0$ in the case of Sio *et al.* and to the polaron level at $q = q^\text{bare}_\text{k}$ in our case. This comparison clarifies the underlying assumptions leading to previous expressions for the SI in the literature. In particular, we remark that when the electron screening is allowed, as in realistic conditions, the SI-corrected energy $E^0(q) + \Delta E^0(q)|_{\text{Sio}}$ no longer satisfies the piece-wise linearity condition. Additional connection to other previous literature [37] is provided in Appendix B.

In Table V, we quantify the differences between the various forms of SI discussed in this paper by comparing the corresponding polaron binding energies. The binding energies free from many-body SI are calculated with the PBE0(α_k) functional [cf. Figs. 3(d)–3(f)]. The binding energies corrected for the one-body SI are obtained by extrapolating the results in Figs. 3(d)–3(f) to the fraction of Fock exchange $\alpha = 1$. The

binding energies corrected for the SI proposed by Sio *et al.* are obtained as

$$E_{\rm f}^0(Q)|_{\rm Sio} = E_{\rm f}^0(Q) + \Delta E^0(Q)|_{\rm Sio}, \tag{58}$$

where $E_{\rm f}^0(Q)$ corresponds to the formation energies at $\alpha = 0$ in Figs. 3(d)–3(f) [cf. Eq. (12)] and $\Delta E^0(Q)|_{\rm Sio}$ is evaluated using the wave functions obtained with PBE0($\alpha_{\rm k}$). As already pointed out in Ref. [47], the binding energies free from one-body SI are considerably larger than those corrected for many-body SI, because of the large shift of the band edges with α [cf. Figs. 3(a)–3(c)]. Moreover, we also find larger values for the formation energies corrected with the scheme of Sio *et al.*, which reflects the neglect of screening effects in Eq. (55).

IV. SEMILOCAL SCHEME FOR POLARON LOCALIZATION

In the previous section, we established the superiority of the many-body SI over the one-body SI. It is of interest to identify a semilocal functional incorporating the many-body SI corrections of the polaron state in a self-consistent calculation. However, as remarked in Ref. [47], the variational minimization of the functional $E^0 + \Delta E^0|_{\rm mb}$ carries some limitations. On the one hand, this would require the knowledge of $q_{\rm k}$, which is inherent to the hybrid-functional calculation, as can be seen in Eq. (24). On the other hand, such a variational implementation would not guarantee polaron localization, since the SI of the valence electron states has not been corrected. For instance, in the case of the hole polaron in MgO, the many-body SI-corrected polaron level $\epsilon_{\rm p}^{\alpha_{\rm k}}$ is situated below the PBE valence band edge [cf. Fig. 3(b)]. The competition between localized and delocalized states prevents polaron localization in this case. Indeed, to achieve polaron localization and a negative formation energy, the polaron level must lie sufficiently deep in the band gap to overcome the energy cost of lattice distortions [cf. Eq. (17)]. For these reasons, we develop an alternative procedure in the following.

A. Methodology

We assume that the localization can be achieved by adding a weak local potential to the PBE Hamiltonian in Eq. (1), which favors the localized state with respect to the delocalized band states. This idea is supported by previous research [101,102], in which the localized and delocalized forms of the polaron state have been found in close energetic competition. We denote this potential V_σ^γ, where γ is a parameter that regulates the strength of the potential. This leads to the following set of equations:

$$\left(\mathcal{H}_\sigma^0 + V_\sigma^\gamma\right)\psi_{i\sigma}^\gamma = \epsilon_{i\sigma}^\gamma \psi_{i\sigma}^\gamma, \tag{59}$$

where $\psi_{i\sigma}^\gamma$ and $\epsilon_{i\sigma}^\gamma$ are the resulting wave functions and eigenvalues, respectively. We find that a suitable expression for V_σ^γ is

$$V_\sigma^\gamma(q) = q\gamma \frac{\partial V_{{\rm xc}\sigma}}{\partial q}. \tag{60}$$

The use of the exchange-correlation potential in the definition of V_σ^γ ensures its locality. Using the chain rule for the derivative of $V_{{\rm xc}\sigma}$ with respect to q and considering Eq. (39), V_σ^γ can be rewritten as

$$V_\sigma^\gamma(q) = -q\gamma \int d\mathbf{r}\, \frac{\delta V_{{\rm xc}\sigma}^0[n_\uparrow^\gamma, n_\downarrow^\gamma]}{\delta n_{\sigma_{\rm p}}^\gamma(\mathbf{r})} n_{\rm p}^\gamma(\mathbf{r}), \tag{61}$$

where n_σ^γ is the total density in the spin channel σ, and $n_{\rm p}^\gamma$ is the density of the polaron state. The dominant contribution to the potential V_σ^γ is given by the exchange term, which only occurs in the spin channel $\sigma = \sigma_{\rm p}$ [cf. Eq. (3)]. For $q = 0$, the potential V_σ^γ vanishes, thus recovering the PBE Hamiltonian.

The structural relaxations are performed in the presence of the polaron charge Q through the usual Hellmann-Feynmann forces, as defined in Eq. (11). We denote the resulting relaxed geometry of the polaron $\mathbf{R}_Q^\gamma$. We remark that the Hellmann-Feynmann theorem and Janak's theorem are still satisfied when introducing the potential V_σ^γ in the Kohn-Sham equations.

We find the value of the parameter $\gamma = \gamma_{\rm k}$ for which the piece-wise linearity of the total energy upon electron occupation is enforced, i.e.,

$$\frac{d}{dq}\epsilon_{\rm p}^\gamma(q)\bigg|_{\gamma=\gamma_{\rm k}} = 0, \tag{62}$$

where $\epsilon_{\rm p}^\gamma$ is the polaron level. In Eq. (62), $\gamma_{\rm k}$ and $\mathbf{R}_Q^{\gamma_{\rm k}}$ are obtained self-consistently. Since the piece-wise linearity condition is satisfied for $\gamma_{\rm k}$, the total energy can be written as

$$E^{\gamma_{\rm k}}(Q) = E^{\gamma_{\rm k}}(0) - Q\epsilon_{\rm p}^{\gamma_{\rm k}}. \tag{63}$$

Therefore, the corresponding polaron formation energy is

$$E_{\rm f}^{\gamma_{\rm k}}(Q) = Q\left(\epsilon_{\rm b}^{\gamma_{\rm k}} - \epsilon_{\rm p}^{\gamma_{\rm k}}\right) + \left(E^{\gamma_{\rm k}}(0) - E_{\rm ref}^{\gamma_{\rm k}}(0)\right). \tag{64}$$

The quantities in Eq. (64) are all calculated at the semilocal level of theory, thus avoiding hybrid functional calculations. Moreover, the band edge $\epsilon_{\rm b}^{\gamma_{\rm k}}$ and the total energies $E^{\gamma_{\rm k}}(0)$ and $E_{\rm ref}^{\gamma_{\rm k}}(0)$ coincide with their respective PBE values, because of the vanishing prefactor q in Eq. (60).

Our semilocal scheme guarantees a symmetric treatment in the case of electron and hole polarons. This stems from the fact that the potential V_σ^γ acts in the same way on all the states, irrespectively of their occupation. Hence, electron and hole polarons, which correspond to the last-occupied and the first-unoccupied Kohn-Sham states, respectively, localize in a analogous manner under the action of this potential.

Our semilocal scheme can be compared with previously proposed methods. The idea that a localized potential might be sufficient for correcting the SI through enforcing the piece-wise linearity condition has previously been used in the DFT+U scheme [103] and in the scheme proposed by Lany and Zunger [37]. In both these schemes, the U correction applies to specific atomic orbitals. At variance, our semilocal method accounting for the many-body SI leads to a localized potential, which self-consistently originates from the electron or hole density and which acts on all the states of the system rather than on selected atomic orbitals.

B. Computational advantages

In practical calculations, the potential V_σ^γ in Eq. (60) can be implemented through finite differences. For an electron

polaron ($q = -1$, $\sigma_p = \uparrow$), we use

$$V_\sigma^\gamma(-1) = \gamma\big(V_{xc\sigma}^0[n_\uparrow^\gamma(-1), n_\downarrow^\gamma(-1)] - V_{xc\sigma}^0[n_\uparrow^\gamma(-1) - n_p^\gamma(-1), n_\downarrow^\gamma(-1)]\big). \quad (65)$$

where the densities are found through self-consistent calculations with $q = -1$. Analogously, for a hole polaron ($q = +1$, $\sigma_p = \downarrow$), we have

$$V_\sigma^\gamma(+1) = \gamma\big(V_{xc\sigma}^0[n_\uparrow^\gamma(+1), n_\downarrow^\gamma(+1)] - V_{xc\sigma}^0[n_\uparrow^\gamma(+1), n_\downarrow^\gamma(+1) + n_p^\gamma(+1)]\big). \quad (66)$$

The expressions in Eqs. (65) and (66) can be easily determined using available exchange-correlation subroutines.

In previous one-body SI schemes [43,44,46], it is common to adopt the ROKS constraint, which consists in setting $\psi_{i\uparrow} = \psi_{i\downarrow}$ for all states. The ROKS condition is useful to avoid multiminima problems encountered in SI-corrected calculations [43,44,46]. However, this approximation enforces the same screening in the two spin channels, which is not generally the case as seen in Fig. 5. This could affect the polaron energetics. At variance, our methodology does not require the ROKS constraint and reaches convergence as fast as standard PBE calculations.

The present semilocal scheme guarantees the orthogonalization of the wave functions without requiring any modification of the available algorithms for the diagonalization of the Hamiltonian, like the Davidson or the conjugate-gradient method. Indeed, the potential V_σ^γ acts as a local potential on all the states in the spin channel σ [cf. Eq. (59)]. This is a great advantage compared to previous SI approaches [42–44,46], which feature orbital-dependent Hamiltonians [41,104–106]. In particular, in the SI correction scheme of Perdew and Zunger [42], a different Hamiltonian acts on each state. In more recent SI methods [43–46], a distinct Hamiltonian is only used for the polaron state. Such orbital-dependent Hamiltonians require more sophisticated diagonalization algorithms [106], which are not necessary in our methodology.

Our approach is only marginally affected by the rotational invariance problem [41,104,105]. We note that the potential V_σ^γ depends on the polaron density n_p^γ. In the case of hole polarons, the occupied manifold preserves the rotational invariance under unitary transformations, since n_p^γ pertains to an unoccupied state. On the other hand, in the case of electron polarons, the rotational invariance is not formally satisfied, since the polaron state is occupied. However, the diagonalization of the Hamiltonian $\mathcal{H}_\sigma^0 + V_\sigma^\gamma$ is only affected to a minor extent because the energy separation between the polaron level and the other occupied levels is generally sizable. This is a great advantage of our methodology compared to previous SI-correction schemes [42–44,46].

The present semilocal scheme has been implemented in the code PW of QUANTUM ESPRESSO [57] and is available to be incorporated in the next official release of the code. In the self-consistent iteration, the polaron density n_p^γ is mixed with the polaron densities at previous steps in the same way as the total electron density [57].

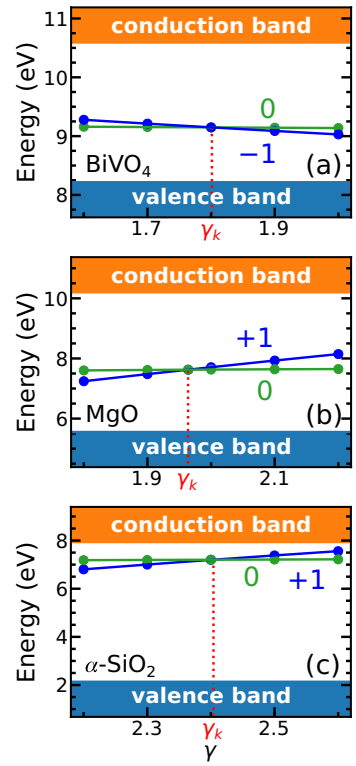

FIG. 7. Polaron energy levels $\epsilon_p^\gamma(Q)$ and $\epsilon_p^\gamma(0)$ for the structure $\mathbf{R}_Q^\gamma$ as a function of γ for the electron polaron in $BiVO_4$, the hole polaron in MgO, and the hole trapped at the Al impurity in α-SiO_2. The polaron levels are identified by their respective polaron charge. The value γ_k is found such that $\epsilon_p^{\gamma_k}(Q) = \epsilon_p^{\gamma_k}(0)$.

C. Semilocal functional results

First, we calculate the value γ_k for which the piece-wise linearity condition is satisfied. Following Eq. (62), we perform structural relaxations for different values of γ and obtain the corresponding polaron geometries $\mathbf{R}_Q^\gamma$. For each structure $\mathbf{R}_Q^\gamma$, we calculate the energy levels $\epsilon_p^\gamma(0)$ and $\epsilon_p^\gamma(Q)$ pertaining to the charge states 0 and Q, as illustrated in Fig. 7. We thus determine γ_k such that those energy levels coincide, resulting in $\gamma_k = 1.80, 1.96, 2.40$ for $BiVO_4$, MgO, and α-SiO_2, respectively. In all cases, the polaron level is situated in the band gap and provides the required electronic energy gain to counterbalance the energy cost of the lattice distortions. This yields stable localized polarons.

We now present the electronic and atomic properties obtained with our semilocal scheme in comparison with the hybrid-functional PBE0(α_k) results. In the two theoretical schemes, we ensure that the calculations are carried out under the same conditions for the accuracy of compliance, the finite-size effects, and the cell size, whereby the differences do not result from such technical aspects. We show in Figs. 8(a) and 8(b) the polaron density integrated over the xy planes, namely,

$$n_p(z) = \int dx dy\, n_p(x, y, z), \quad (67)$$

and find an excellent agreement between the two schemes. To compare the polaron structures, we report in Table VI the lengths of the distorted bonds. For all investigated

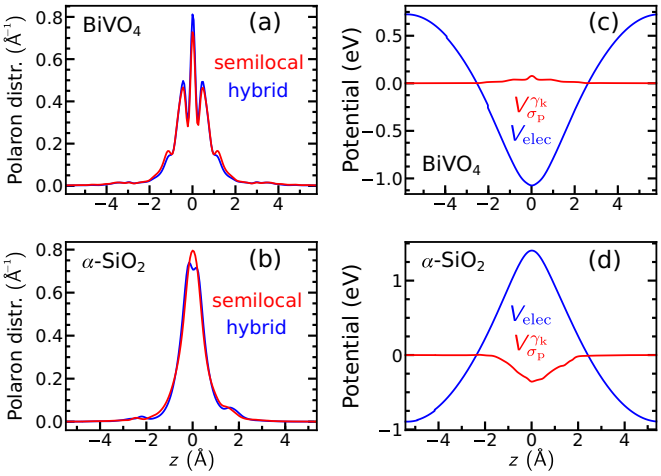

FIG. 8. [(a), (b)] Polaron densities for the electron polaron in $BiVO_4$ and for the hole trapped at the Al impurity in α-SiO_2 as obtained with the hybrid functional PBE0(α_k) and with the semilocal scheme introduced in this paper. The polaron densities are integrated over xy planes. [(c),(d)] Electrostatic potential $V_{\rm elec} = V_{\rm H}[Qn_{\rm p}^{\gamma_k}]$ and potential $V_{\sigma_p}^{\gamma_k}(Q)$ averaged over xy planes ($Q = -1$ for electron polarons, $Q = +1$ for hole polarons). The results for the hole polaron in MgO are shown in Ref. [47].

polarons, the agreement between the semilocal and the hybrid-functional values is very good. The differences are all within 0.03 Å, except for the weak Al-O bond in α-SiO_2, which differs by 0.12 Å.

Next, we determine the polaron formation energies and give the results in Table VII. With our semilocal scheme, we find formation energies of −0.44 eV, −0.50 eV, and −2.75 eV for $BiVO_4$, MgO, and α-SiO_2, respectively. These values differ from the hybrid functional values by 0.19, 0.03, and 0.36 eV, respectively. This agreement is remarkable given the large differences in formation energies found as a function of α in Figs. 3(d)–3(f). Furthermore, this agreement suggests that enforcing the piece-wise linearity condition leads to robust polaron formation energies, irrespective of the choice of the functional.

The semilocal scheme allows one to carry out convergence tests with cell size and **k**-point sampling overcoming computational limitations inherent to hybrid-functional calculations. We calculate the polaron formation energy for larger supercell

TABLE VI. Bond lengths (in Å) of the distorted polaronic structures ($q = Q$) as obtained with the hybrid functional PBE0(α_k) and with the semilocal scheme introduced in this paper. For α-SiO_2, we give the lengths of the short/long Al-O bonds. For reference, we also report the corresponding bond lengths as obtained with PBE in the absence of the polaron ($q = 0$).

	$q = 0$	$q = Q$	
System	PBE	Semilocal	Hybrid
$BiVO_4$	1.73	1.82	1.80
MgO	2.11	2.23	2.20
α-SiO_2	1.74/1.74	1.71/2.03	1.69/1.91

TABLE VII. Polaron formation energy obtained with the hybrid functional PBE0(α_k) and with the semilocal scheme introduced in this study. Energies are in eV.

	Semilocal	Hybrid
$BiVO_4$	−0.44	−0.63
MgO	−0.50	−0.53
α-SiO_2	−2.75	−3.11

sizes and finer **k**-point sampling for the three systems studied in this study, as given in Table VIII. The converged results deviate by at most 0.07 eV from the results in Table VII. This further corroborates the accuracy of the employed finite-size correction scheme [75]. For the electron polaron in $BiVO_4$, we calculate with $\alpha_k = 0.14$ a converged formation energy of −0.38 eV, to be compared with the value of −1.09 eV obtained in Ref. [26] with $\alpha = 0.22$ and with a different electronic-structure set-up. This is consistent with the variation of the formation energy by −0.65 eV when α increases from 0.14 to 0.22, as can seen in Fig. 3(d). For the hole polaron in MgO, the converged formation energy with $\alpha_k = 0.34$ is found to be −0.49 eV, in good agreement with the value of −0.38 eV found in Ref. [75] with a different electronic structure set-up and with $\alpha = 0.33$. Accounting for the variation of the formation energy when α goes from 0.33 to 0.34 [cf. Fig. 3(e)], reduces the discrepancy to only 0.04 eV.

It is of interest to remark that the formation energies obtained in our semilocal scheme are close to the PBE0(α_k) values, despite the fact that the band gaps are underestimated like in PBE. This can be understood by considering that the polaron states of interest in our study are mainly constructed with band states to which the polaron belongs, i.e., conduction band states for electron polarons and valence band states for hole polarons. In such conditions, the description of the band gap is thus not a stringent requirement for achieving accurate formation energies.

In the case of MgO, the robustness of the results for the self-trapped hole polaron is of particular interest. Indeed, the experimental situation concerning the self-trapped hole remains difficult to interpret in a clear way [9,107] and the theoretical description is controversial [24,33,75,108]. In these regards, the hybrid-functional and semilocal schemes with

TABLE VIII. Polaron formation energies $E_f^{\gamma_k}$ as calculated with the semilocal scheme for various supercell sizes and **k**-point samplings.

System	Number of atoms	**k**-point grid	$E_f^{\gamma_k}$
$BiVO_4$	96	Γ	−0.44
	96	2×2×2	−0.36
	216	2×2×2	−0.38
MgO	64	Γ	−0.50
	64	2×2×2	−0.49
	512	2×2×2	−0.49
α-SiO_2	64	Γ	−2.75
	64	2×2×2	−2.69
	243	2×2×2	−2.68

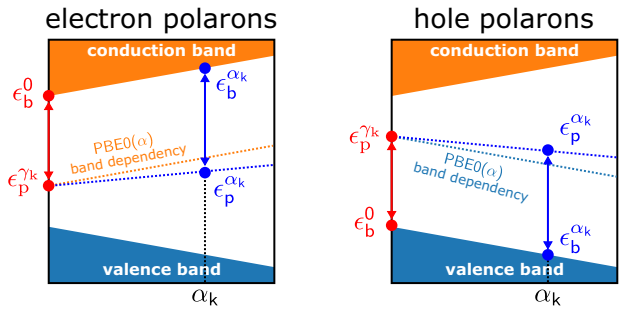

FIG. 9. Graphical representation related to Eq. (71) to show the robustness of polaron formation energies obtained with semilocal and hybrid functional approaches.

vanishing many-body self-interaction consistently predict a self-trapped hole with almost identical formation energy (see Table VII).

It is important to formally investigate the relationship between the formation energies obtained with the semilocal and hybrid functional schemes. Indeed, the piece-wise linearity in these functionals is achieved in remarkably different ways, either through the local potential $V_\sigma^{\gamma_k}$ or through the nonlocal Fock exchange terms. The difference between the formation energies in Eqs. (17) and (64) can be expressed as

$$E_f^{\alpha_k}(Q) - E_f^{\gamma_k}(Q) = Q\left(\epsilon_b^{\alpha_k} - \epsilon_b^0\right) - Q\left(\epsilon_p^{\alpha_k} - \epsilon_p^{\gamma_k}\right), \quad (68)$$

where we focus on the electronic gain due to localization, assuming that the cost of lattice distortions is similar in the two schemes. Given the linear dependence of the band-edge levels with α [cf. Figs. 3(a)–3(c)], the band contributions in Eq. (68) can be expanded in α as

$$\epsilon_b^{\alpha_k} - \epsilon_b^0 = \alpha_k \frac{d\epsilon_b^\alpha}{d\alpha}. \quad (69)$$

Moreover, using the linearity of the polaron level with α [cf. Figs. 3(a)–3(c)], the polaron terms in Eq. (68) can be rewritten as

$$\epsilon_p^{\alpha_k} - \epsilon_p^{\gamma_k} = \epsilon_p^{\alpha_k}(0) - \epsilon_p^0(0) = \alpha_k \frac{d\epsilon_p^\alpha(0)}{d\alpha}, \quad (70)$$

where we used the facts that $\epsilon_p^{\alpha_k}$ and $\epsilon_p^{\gamma_k}$ are constant with q and that $\epsilon_p^{\gamma_k} = \epsilon_p^0(0)$ due to the presence of the prefactor q in $V_\sigma^{\gamma_k}$ [cf. Eq. (60)]. Hence, through the use of Eqs. (69) and (70), Eq. (68) becomes

$$E_f^{\alpha_k}(Q) - E_f^{\gamma_k}(Q) = Q\alpha_k\left[\frac{d\epsilon_b^\alpha}{d\alpha} - \frac{d\epsilon_p^0(0)}{d\alpha}\right]. \quad (71)$$

This expression indicates that when the piece-wise linearity is satisfied the formation energies obtained with semilocal and hybrid functionals coincide, provided that the polaron level at $q = 0$ and the associated band edge vary with α in the same way. This condition is generally closely satisfied because these states belong to the same electronic manifold. A schematical representation of Eq. (71) is given in Fig. 9. This analysis emphasizes the robustness of the polaron formation energies achieved through the enforcement of the piece-wise linearity, irrespective of the detailed features of the employed functional.

We verify that $V_\sigma^{\gamma_k}(Q)$ is indeed a weak potential. For this purpose, we compare $V_{\sigma_p}^{\gamma_k}(Q)$ and the electrostatic potential $V_H[Qn_p^{\gamma_k}]$ generated by the polaron charge density $Qn_p^{\gamma_k}$, where $Q = -1$ for electron polarons and $Q = +1$ for hole polarons. In Figs. 8(c) and 8(d), we show these potentials averaged over xy planes as a function of the z coordinate, namely,

$$V(z) = \frac{1}{\mathcal{A}_{xy}} \int dx dy\, V(x, y, z), \quad (72)$$

where $\mathcal{A}_{xy}$ denotes the area of xy planes in the supercell. In all cases, we find that the potential $V_{\sigma_p}^{\gamma_k}(Q)$ is considerably weaker than the electrostatic potential. Moreover, the peak of the potential $V_{\sigma_p}^{\gamma_k}(Q)$ amounts to a small fraction of an electronvolt [cf. Figs. 8(c) and 8(d)]. This confirms *a posteriori* that the polaron can be localized by adding a weak potential to the PBE Hamiltonian. Additionally, we remark that the potential $V_{\sigma_p}^{\gamma_k}(Q)$ carries an opposite sign with respect to the electrostatic potential. To understand this property, let us focus on the case of electron polarons [e.g., in $BiVO_4$, Fig. 8(c)]. The electrostatic potential $V_H[-n_p^{\gamma_k}]$ generated by the polaron charge density results in a potential well, which repels the negative charge of the electron polaron. Hence, $V_H[-n_p^{\gamma_k}]$ tends to delocalize the electron polaron charge density. The potential $V_{\sigma_p}^{\gamma_k}(Q)$ opposes this electrostatic potential, thereby favoring polaron localization. A similar reasoning applies to the case of hole polarons.

V. CONCLUSIONS

In this paper, we first develop a unified theoretical formulation encompassing many-body and one-body forms of self-interaction. We find an analytic expression for both forms of self-interaction and highlight their connection in terms of the dielectric constant. In particular, the two forms of self-interaction are found to coincide when the electron screening is turned off. This analysis thus confers superiority to the notion of many-body self-interaction with respect to that of one-body self-interaction. Second, we address the many-body self-interaction of polarons at the semilocal level of theory. Polaron localization is achieved by the inclusion of a weak local potential in the Kohn-Sham Hamiltonian that enforces the piece-wise linearity of the total energy upon electron occupation. Our methodology is particularly advantageous from the computational point of view. In particular, it does not entail any computational overhead compared to regular semilocal calculations, does not suffer from diagonalization problems related to orbital-dependent Hamiltonians, and avoids the use of the ROKS constraint. The resulting structural and electronic properties are in agreement with those of a hybrid functional satisfying the same constraint. This agreement suggests that the suppression of the many-body self-interaction leads to polaron properties that are robust with respect to the adopted functional. This is expected to hold also in the case of competitive polaronic states at surfaces [109] or in amorphous materials [110].

Our paper shows that implementing a constraint like the piece-wise linearity from exact density functional theory in approximate functionals results in a successful description of the self-interaction. Following the same lines, one could also specifically focus on including the long-range $-1/(\varepsilon_\infty r)$

dependence of the Coulomb potential [91], which is another property of the exact density functional [39]. In PBE0(α) functionals, these properties correspond to setting the fraction of Fock exchange to α_k and $\alpha_{lr} = 1/\varepsilon_\infty$, respectively. For most materials, the values of α_k and α_{lr} are generally quite close, leading to similar band gaps [25,63]. When α_k and α_{lr} differ noticeably, it is still possible to include both conditions coming from exact density functional theory through the consideration of more involved functionals, such as range-separated hybrid functionals [25,65,91,96].

To conclude, our paper advances the conceptual understanding of the self-interaction problem in density functional theory. This paves the way to efficient calculations of polarons in large systems, in systematic studies involving large sets of materials, and in molecular dynamics evolving over long time periods.

ACKNOWLEDGMENTS

This work has been realized in relation to the National Center of Competence in Research (NCCR) "Materials' Revolution: Computational Design and Discovery of Novel Materials (MARVEL)" of the SNSF (Grant No. 182892). The calculations have been performed at the Swiss National Supercomputing Centre (CSCS) (Grant under Projects ID s1125 and ID mr25). Material associated with this paper can be found on Materials Cloud [111].

APPENDIX A: ASSUMPTIONS OF THE UNIFIED THEORETICAL FRAMEWORK FOR THE SELF-INTERACTION

In our unified theoretical formulation for the self-interaction (cf. Sec. III A), the polaron level $\epsilon_p^\alpha(q)$ is assumed to be linear in q and in α. This assumption has implications on the wave functions $\psi_{i\sigma}^\alpha$, which we discuss here in detail.

We first focus on the assumption of linearity of $\epsilon_p^\alpha(q)$ with respect to q. Then, the first derivative of $\epsilon_p^\alpha(q)$ with respect to q must be a constant. For simplicity, we consider the case $\alpha = 0$. Using the Hellmann-Feynman theorem and the chain rule for the derivatives with respect to q, we get

$$\begin{aligned}\frac{d\epsilon_p^0(q)}{dq} &= \langle\psi_p^0|\frac{d\mathcal{H}_{\sigma_p}^0}{dq}|\psi_p^0\rangle \\ &= \sum_\sigma \int d\mathbf{r}d\mathbf{r}' \frac{\delta\mathcal{H}_{\sigma_p}^0[n_\uparrow^0, n_\downarrow^0](\mathbf{r})}{\delta n_\sigma^0(\mathbf{r}')}\frac{dn_\sigma^0(\mathbf{r}')}{dq}n_p^0(\mathbf{r}). \quad \text{(A1)}\end{aligned}$$

We note that the derivative dn_σ^0/dq can be split into contributions pertaining to the polaron and to the valence electrons. Using the definition of the density of valence electrons in Eq. (39), we can write

$$\frac{dn_\sigma^0}{dq} = \frac{dn_{\sigma\,\mathrm{val}}^0}{dq} - \delta_{\sigma,\sigma_p}\left(n_p^0 + q\frac{dn_p^0}{dq}\right). \quad \text{(A2)}$$

By inserting Eq. (A2) in Eq. (A1), one infers that $d\epsilon_p^0(q)/dq$ is constant with q when neglecting the variations of the polaron density with q and the second-order derivative of the valence electron density with respect to q, i.e.,

$$\frac{dn_p^0}{dq} = 0 \qquad \text{and} \qquad \frac{d^2n_{\sigma\,\mathrm{val}}^0}{dq^2} = 0. \quad \text{(A3)}$$

Such conditions also apply to the respective wave functions and can be extended to the case $\alpha \neq 0$.

Next, we consider the assumption of linearity of $\epsilon_p^\alpha(q)$ in α. Then, the first derivative of $\epsilon_p^\alpha(q)$ with respect to α must be a constant. Using the Hellmann-Feynman theorem and expliciting the α dependency of the Hamiltonian $\mathcal{H}_{\sigma_p}^\alpha$, one has

$$\begin{aligned}\frac{d\epsilon_p^\alpha(q)}{d\alpha} &= \langle\psi_p^\alpha|\frac{d\mathcal{H}_{\sigma_p}^\alpha}{d\alpha}|\psi_p^\alpha\rangle \\ &= \langle\psi_p^\alpha|\frac{d}{d\alpha}\left(\mathcal{H}_{\sigma_p}^0 + \alpha\frac{\partial\mathcal{H}_{\sigma_p}^\alpha}{\partial\alpha}\right)|\psi_p^\alpha\rangle \\ &= \langle\psi_p^\alpha|\left(\frac{d\mathcal{H}_{\sigma_p}^0}{d\alpha} + \frac{\partial\mathcal{H}_{\sigma_p}^\alpha}{\partial\alpha} + \alpha\frac{d}{d\alpha}\frac{\partial\mathcal{H}_{\sigma_p}^\alpha}{\partial\alpha}\right)|\psi_p^\alpha\rangle. \quad \text{(A4)}\end{aligned}$$

Then, neglecting the explicit α-dependent term in Eq. (A4), one obtains

$$\frac{d\epsilon_p^\alpha(q)}{d\alpha} = \langle\psi_p^\alpha|\left(\frac{d\mathcal{H}_{\sigma_p}^0}{d\alpha} + \frac{\partial\mathcal{H}_{\sigma_p}^\alpha}{\partial\alpha}\right)|\psi_p^\alpha\rangle, \quad \text{(A5)}$$

where

$$\frac{d\mathcal{H}_{\sigma_p}^0}{d\alpha} = \sum_\sigma \int d\mathbf{r}\,\frac{\delta\mathcal{H}_{\sigma_p}^0[n_\uparrow^\alpha, n_\downarrow^\alpha]}{\delta n_\sigma^\alpha(\mathbf{r})}\frac{dn_\sigma^\alpha(\mathbf{r})}{dq}, \quad \text{(A6)}$$

and

$$\frac{\partial\mathcal{H}_{\sigma_p}^\alpha}{\partial\alpha} = -V_{x\sigma_p}[n_\uparrow^\alpha, n_\downarrow^\alpha] + V_x[\{\psi_{i\sigma_p}^\alpha\}]. \quad \text{(A7)}$$

Thus, Eq. (A5) depends on α only through the wave functions $\psi_{i\sigma}^\alpha$. Therefore, the assumption of constant $d\epsilon_p^\alpha(q)/d\alpha$ with α implies neglecting the variations of the wave functions with α, i.e.,

$$\frac{d\psi_{i\sigma}^\alpha}{d\alpha} = 0. \quad \text{(A8)}$$

APPENDIX B: CONNECTION WITH OTHER PREVIOUS LITERATURE

Following Ref. [37], the electron addition energy can be expressed in our notation as

$$E^\alpha(q) - E^\alpha(0) = -q\epsilon_p^\alpha(0) + \Pi_p^\alpha(q) + \Sigma_p^\alpha(q), \quad \text{(B1)}$$

where Π_p^α is defined as SI energy of the polaron in the absence of electron screening, and Σ_p^α is the energy contribution arising from wave-function relaxation. We here find the expression of Π_p^α and Σ_p^α within our formulation. We start by expanding the total energy $E^\alpha(q)$ in q around $q = 0$,

$$\begin{aligned}E^\alpha(q) - E^\alpha(0) &= q\frac{dE^\alpha(q)}{dq}\bigg|_0 + \frac{q^2}{2}\frac{d^2E^\alpha(q)}{dq^2} \\ &= -q\epsilon_p^\alpha(0) + \frac{q^2}{2}\frac{d^2E^\alpha(q)}{dq^2}, \quad \text{(B2)}\end{aligned}$$

where we used Janak's theorem. Next, we split the second-order derivative of $E^\alpha(q)$ with respect to q into bare and

screening contributions, namely,

$$\frac{d^2E^\alpha(q)}{dq^2} = \left.\frac{d^2E^\alpha(q)}{dq^2}\right|_{\text{bare}} + \left(\frac{d^2E^\alpha(q)}{dq^2} - \left.\frac{d^2E^\alpha(q)}{dq^2}\right|_{\text{bare}}\right). \tag{B3}$$

We remark that

$$\frac{d^2E^\alpha(q)}{dq^2} = \left(1 - \frac{\alpha}{\alpha_k}\right)\frac{d^2E^0(q)}{dq^2}, \tag{B4}$$

and that, similarly to Eq. (53),

$$\left.\frac{d^2E^\alpha(q)}{dq^2}\right|_{\text{bare}} = (1-\alpha)\left.\frac{d^2E^0(q)}{dq^2}\right|_{\text{bare}}. \tag{B5}$$

Then, comparing Eqs. (B1) and (B2), and using Eq. (55), one identifies the following expressions for Π_p^α and Σ_p^α:

$$\Pi_p^\alpha(q) = \frac{1}{2}(1-\alpha)q^2\left.\frac{d^2E^0(q)}{dq^2}\right|_{\text{bare}} = (1-\alpha)\,\Delta E^0(q)\big|_{\text{Sio}}, \tag{B6}$$

$$\Sigma_p^\alpha(q) = \frac{1}{2}\left(1 - \frac{\alpha}{\alpha_k}\right)q^2\frac{d^2E^0(q)}{dq^2} - (1-\alpha)\,\Delta E^0(q)\big|_{\text{Sio}}. \tag{B7}$$

Through our formulation, we thus find a connection between the approaches in Ref. [37] and Refs. [45,46].

[1] C. Franchini, M. Reticcioli, M. Setvin, and U. Diebold, Nat. Rev. Mater **6**, 560 (2021).
[2] S. Moser, L. Moreschini, J. Jaćimović, O. S. Barišić, H. Berger, A. Magrez, Y. J. Chang, K. S. Kim, A. Bostwick, E. Rotenberg, L. Forró, and M. Grioni, Phys. Rev. Lett. **110**, 196403 (2013).
[3] C. Cancellieri, A. S. Mishchenko, U. Aschauer, A. Filippetti, C. Faber, O. Barišić, V. Rogalev, T. Schmitt, N. Nagaosa, and V. N. Strocov, Nat. Commun. **7**, 10386 (2016).
[4] Z. Wang, S. M. Walker, A. Tamai, Y. Wang, Z. Ristic, F. Y. Bruno, A. De La Torre, S. Riccò, N. Plumb, M. Shi *et al.*, Nat. Mater. **15**, 835 (2016).
[5] O. Schirmer, Solid State Commun. **18**, 1349 (1976).
[6] T. J. L. Jenkin, J. Koppitz, O. F. Schirmer, and W. Hayes, J. Phys. C **20**, L367 (1987).
[7] S. Yang, A. T. Brant, and L. E. Halliburton, Phys. Rev. B **82**, 035209 (2010).
[8] T. Harwig and F. Kellendonk, J. Solid State Chem. **24**, 255 (1978).
[9] Z. A. Rachko and J. A. Valbis, Phys. Status Solidi B **93**, 161 (1979).
[10] B. Namozov, M. Fominich, R. Zakharchenya, and V. Myurk, Phys. Solid State **40**, 837 (1998).
[11] C. Itoh, K. Tanimura, N. Itoh, and M. Itoh, Phys. Rev. B **39**, 11183 (1989).
[12] M. Kang, S. W. Jung, W. J. Shin, Y. Sohn, S. H. Ryu, T. K. Kim, M. Hoesch, and K. S. Kim, Nat. Mater. **17**, 676 (2018).
[13] C. Chen, J. Avila, E. Frantzeskakis, A. Levy, and M. C. Asensio, Nat. Commun. **6**, 1 (2015).
[14] C. Chen, J. Avila, S. Wang, Y. Wang, M. Mucha-Kruczynski, C. Shen, R. Yang, B. Nosarzewski, T. P. Devereaux, G. Zhang *et al.*, Nano Lett. **18**, 1082 (2018).
[15] M. Reticcioli, U. Diebold, G. Kresse, and C. Franchini, in *Handbook of Materials Modeling: Applications: Current and Emerging Materials*, edited by W. Andreoni and S. Yip (Springer, Cham, 2020) pp. 1035.
[16] L. D. Landau, Phys. Z. Sowjetunion **3**, 664 (1933).
[17] S. I. Pekar, Zh. Eksp. Teor. Fiz **16**, 341 (1946).
[18] L. D. Landau and S. I. Pekar, Zh. Eksp. Teor. Fiz **18**, 419 (1948).
[19] H. Fröhlich, H. Pelzer, and S. Zienau, London, Edinburgh Dublin Philos. Mag. J. Sci. **41**, 221 (1950).
[20] T. Holstein, Ann. Phys. **8**, 325 (1959).
[21] N. V. Prokof'ev and B. V. Svistunov, Phys. Rev. Lett. **81**, 2514 (1998).
[22] J. T. Titantah, C. Pierleoni, and S. Ciuchi, Phys. Rev. Lett. **87**, 206406 (2001).
[23] F. Grusdt, Phys. Rev. B **93**, 144302 (2016).
[24] J. B. Varley, A. Janotti, C. Franchini, and C. G. Van de Walle, Phys. Rev. B **85**, 081109(R) (2012).
[25] G. Miceli, W. Chen, I. Reshetnyak, and A. Pasquarello, Phys. Rev. B **97**, 121112(R) (2018).
[26] J. Wiktor, F. Ambrosio, and A. Pasquarello, ACS Energy Lett. **3**, 1693 (2018).
[27] J. Wiktor and A. Pasquarello, ACS Appl. Mater. Interfaces **11**, 18423 (2019).
[28] N. Österbacka, P. Erhart, S. Falletta, A. Pasquarello, and J. Wiktor, Chem. Mater. **32**, 8393 (2020).
[29] M.-H. Du and S. B. Zhang, Phys. Rev. B **80**, 115217 (2009).
[30] P. Deák, B. Aradi, and T. Frauenheim, Phys. Rev. B **83**, 155207 (2011).
[31] C. Spreafico and J. VandeVondele, Phys. Chem. Chem. Phys. **16**, 26144 (2014).
[32] S. Lany, Phys. Status Solidi B **248**, 1052 (2011).
[33] S. Kokott, S. V. Levchenko, P. Rinke, and M. Scheffler, New J. Phys. **20**, 033023 (2018).
[34] J. P. Perdew, K. Burke, and M. Ernzerhof, Phys. Rev. Lett. **77**, 3865 (1996).
[35] T. Schmidt and S. Kümmel, Phys. Rev. B **93**, 165120 (2016).
[36] P. Mori-Sánchez, A. J. Cohen, and W. Yang, J. Chem. Phys. **125**, 201102 (2006).
[37] S. Lany and A. Zunger, Phys. Rev. B **80**, 085202 (2009).
[38] A. Ruzsinszky, J. P. Perdew, G. I. Csonka, O. A. Vydrov, and G. E. Scuseria, J. Chem. Phys. **125**, 194112 (2006).
[39] L. Kronik and S. Kümmel, Phys. Chem. Chem. Phys. **22**, 16467 (2020).
[40] V. Atalla, I. Y. Zhang, O. T. Hofmann, X. Ren, P. Rinke, and M. Scheffler, Phys. Rev. B **94**, 035140 (2016).
[41] T. Körzdörfer, S. Kümmel, and M. Mundt, J. Chem. Phys. **129**, 014110 (2008).
[42] J. P. Perdew and A. Zunger, Phys. Rev. B **23**, 5048 (1981).
[43] M. d'Avezac, M. Calandra, and F. Mauri, Phys. Rev. B **71**, 205210 (2005).
[44] J. VandeVondele and M. Sprik, Phys. Chem. Chem. Phys. **7**, 1363 (2005).

[45] W. H. Sio, C. Verdi, S. Poncé, and F. Giustino, Phys. Rev. Lett. **122**, 246403 (2019).

[46] W. H. Sio, C. Verdi, S. Poncé, and F. Giustino, Phys. Rev. B **99**, 235139 (2019).

[47] S. Falletta and A. Pasquarello, Phys. Rev. Lett. **129**, 126401 (2022).

[48] E. M. Dianov, V. N. Karpechev, V. O. Sokolov, V. B. Sulimov, P. V. Chernov, L. S. Kornienko, I. O. Morozova, and A. O. Rybaltovskii, Phys. Status Solidi B **156**, 663 (1989).

[49] F. Illas and G. Pacchioni, J. Chem. Phys. **108**, 7835 (1998).

[50] G. Pacchioni and A. Basile, Phys. Rev. B **60**, 9990 (1999).

[51] G. Pacchioni, F. Frigoli, D. Ricci, and J. A. Weil, Phys. Rev. B **63**, 054102 (2000).

[52] J. Lægsgaard and K. Stokbro, Phys. Rev. Lett. **86**, 2834 (2001).

[53] S. Sicolo, G. Palma, C. Di Valentin, and G. Pacchioni, Phys. Rev. B **76**, 075121 (2007).

[54] R. Dovesi, V. R. Saunders, C. Roetti, R. Orlando, C. Zicovich-Wilson, F. Pascale, B. Civalleri, K. Doll, N. M. Harrison, I. J. Bush *et al.* (University of Torino, Torino, Italy, 2006)

[55] J. VandeVondele, M. Krack, F. Mohamed, M. Parrinello, T. Chassaing, and J. Hutter, Comput. Phys. Commun. **167**, 103 (2005).

[56] G. Kresse and J. Furthmüller, Phys. Rev. B **54**, 11169 (1996).

[57] P. Giannozzi, S. Baroni, N. Bonini, M. Calandra, R. Car, C. Cavazzoni, D. Ceresoli, G. L. Chiarotti, M. Cococcioni, I. Dabo *et al.*, J. Phys.: Condens. Matter **21**, 395502 (2009).

[58] X. Gonze, J.-M. Beuken, R. Caracas, F. Detraux, M. Fuchs, G.-M. Rignanese, L. Sindic, M. Verstraete, G. Zerah, F. Jollet *et al.*, Comput. Mater. Sci. **25**, 478 (2002).

[59] P. Deák, Q. Duy Ho, F. Seemann, B. Aradi, M. Lorke, and T. Frauenheim, Phys. Rev. B **95**, 075208 (2017).

[60] B. Sadigh, P. Erhart, and D. Åberg, Phys. Rev. B **92**, 075202 (2015).

[61] N. Sai, P. F. Barbara, and K. Leung, Phys. Rev. Lett. **106**, 226403 (2011).

[62] S. Refaely-Abramson, S. Sharifzadeh, M. Jain, R. Baer, J. B. Neaton, and L. Kronik, Phys. Rev. B **88**, 081204(R) (2013).

[63] T. Bischoff, J. Wiktor, W. Chen, and A. Pasquarello, Phys. Rev. Materials **3**, 123802 (2019).

[64] T. Bischoff, I. Reshetnyak, and A. Pasquarello, Phys. Rev. B **99**, 201114(R) (2019).

[65] T. Bischoff, I. Reshetnyak, and A. Pasquarello, Phys. Rev. Research **3**, 023182 (2021).

[66] J. Yang, S. Falletta, and A. Pasquarello, J. Phys. Chem. Lett. **13**, 3066 (2022).

[67] G. L. Oliver and J. P. Perdew, Phys. Rev. A **20**, 397 (1979).

[68] J. P. Perdew, M. Ernzerhof, and K. Burke, J. Chem. Phys. **105**, 9982 (1996).

[69] P. Pulay, Mol. Phys. **17**, 197 (1969).

[70] C. Freysoldt, B. Grabowski, T. Hickel, J. Neugebauer, G. Kresse, A. Janotti, and C. G. Van de Walle, Rev. Mod. Phys. **86**, 253 (2014).

[71] H.-P. Komsa, T. T. Rantala, and A. Pasquarello, Phys. Rev. B **86**, 045112 (2012).

[72] J. F. Janak, Phys. Rev. B **18**, 7165 (1978).

[73] C. Freysoldt, J. Neugebauer, and C. G. Van de Walle, Phys. Rev. Lett. **102**, 016402 (2009).

[74] C. Freysoldt, J. Neugebauer, and C. G. Van de Walle, Phys. Status Solidi B **248**, 1067 (2011).

[75] S. Falletta, J. Wiktor, and A. Pasquarello, Phys. Rev. B **102**, 041115(R) (2020).

[76] P. Umari and A. Pasquarello, Phys. Rev. Lett. **89**, 157602 (2002).

[77] M. van Setten, M. Giantomassi, E. Bousquet, M. Verstraete, D. Hamann, X. Gonze, and G.-M. Rignanese, Comput. Phys. Commun. **226**, 39 (2018).

[78] M. Gerosa, C. Di Valentin, C. E. Bottani, G. Onida, and G. Pacchioni, J. Chem. Phys. **143**, 111103 (2015).

[79] D. Han, D. West, X.-B. Li, S.-Y. Xie, H.-B. Sun, and S. B. Zhang, Phys. Rev. B **82**, 155132 (2010).

[80] J. Wiktor, I. Reshetnyak, F. Ambrosio, and A. Pasquarello, Phys. Rev. Materials **1**, 022401(R) (2017).

[81] K. Sayama, A. Nomura, T. Arai, T. Sugita, R. Abe, M. Yanagida, T. Oi, Y. Iwasaki, Y. Abe, and H. Sugihara, J. Phys. Chem. B **110**, 11352 (2006).

[82] H. Luo, A. H. Mueller, T. M. McCleskey, A. K. Burrell, E. Bauer, and Q. X. Jia, J. Phys. Chem. C **112**, 6099 (2008).

[83] A. Kudo, K. Omori, and H. Kato, J. Am. Chem. Soc. **121**, 11459 (1999).

[84] J. P. Nery, P. B. Allen, G. Antonius, L. Reining, A. Miglio, and X. Gonze, Phys. Rev. B **97**, 115145 (2018).

[85] T. Onuma, W. Kosaka, K. Kudo, Y. Ota, T. Yamaguchi, K. Kaneko, S. Fujita, and T. Honda, Appl. Phys. Lett. **119**, 132105 (2021).

[86] G. Kresse, M. Marsman, L. E. Hintzsche, and E. Flage-Larsen, Phys. Rev. B **85**, 045205 (2012).

[87] M. Engel, H. Miranda, L. Chaput, A. Togo, C. Verdi, M. Marsman, and G. Kresse, arXiv:2205.04265.

[88] H. Philipp, Solid State Commun. **4**, 73 (1966).

[89] J. Wiktor, I. Reshetnyak, M. Strach, M. Scarongella, R. Buonsanti, and A. Pasquarello, J. Phys. Chem. Lett. **9**, 5698 (2018).

[90] G. Capano, F. Ambrosio, S. Kampouri, K. C. Stylianou, A. Pasquarello, and B. Smit, J. Phys. Chem. C **124**, 4065 (2020).

[91] D. Wing, J. Strand, T. Durrant, A. L. Shluger, and L. Kronik, Phys. Rev. Materials **4**, 083808 (2020).

[92] D. Wing, G. Ohad, J. B. Haber, M. R. Filip, S. E. Gant, J. B. Neaton, and L. Kronik, Proc. Natl. Acad. Sci. USA **118**, e2104556118 (2021).

[93] T. J. Smart, F. Wu, M. Govoni, and Y. Ping, Phys. Rev. Mater. **2**, 124002 (2018).

[94] A. Alkauskas, P. Broqvist, and A. Pasquarello, Phys. Status Solidi B **248**, 775 (2011).

[95] M. A. L. Marques, J. Vidal, M. J. T. Oliveira, L. Reining, and S. Botti, Phys. Rev. B **83**, 035119 (2011).

[96] S. Refaely-Abramson, M. Jain, S. Sharifzadeh, J. B. Neaton, and L. Kronik, Phys. Rev. B **92**, 081204(R) (2015).

[97] J. H. Skone, M. Govoni, and G. Galli, Phys. Rev. B **89**, 195112 (2014).

[98] W. Chen, G. Miceli, G.-M. Rignanese, and A. Pasquarello, Phys. Rev. Materials **2**, 073803 (2018).

[99] F. Bassani, G. P. Parravicini, R. A. Ballinger, and J. L. Birman, Phys. Today **29**(3), 58 (1976).

[100] T. M. Henderson, J. Paier, and G. E. Scuseria, Phys. Status Solidi (b) **248**, 767 (2011).

[101] J. L. Gavartin, P. V. Sushko, and A. L. Shluger, Phys. Rev. B **67**, 035108 (2003).

[102] A. Carvalho, A. Alkauskas, A. Pasquarello, A. K. Tagantsev, and N. Setter, Phys. Rev. B **80**, 195205 (2009).

[103] M. Cococcioni and S. de Gironcoli, Phys. Rev. B **71**, 035105 (2005).
[104] S. Kümmel and L. Kronik, Rev. Mod. Phys. **80**, 3 (2008).
[105] S. Klüpfel, P. Klüpfel, and H. Jónsson, J. Chem. Phys. **137**, 124102 (2012).
[106] G. Borghi, C.-H. Park, N. L. Nguyen, A. Ferretti, and N. Marzari, Phys. Rev. B **91**, 155112 (2015).
[107] S. Dolgov, T. Kärner, A. Lushchik, A. Maaroos, S. Nakonechnyi, and E. Shablonin, Phys. Solid State **53**, 1244 (2011).
[108] A. L. Shluger, E. N. Heifets, J. D. Gale, and C. R. A. Catlow, J. Phys.: Condens. Matter **4**, 5711 (1992).
[109] M. V. Ganduglia-Pirovano, J. L. F. Da Silva, and J. Sauer, Phys. Rev. Lett. **102**, 026101 (2009).
[110] A. L. Shluger, K. P. McKenna, P. V. Sushko, D. M. Ramo, and A. V. Kimmel, Modell. Simul. Mater. Sci. Eng. **17**, 084004 (2009).
[111] S. Falletta and A. Pasquarello, doi: 10.24435/materialscloud:7p-gy (2022).